

Accepted Article

Title: In Situ and Operando Techniques for Investigating Electron Transfer in Biological Systems

Authors: João Carlos Perbone de Souza, Lucyano J. A. Macedo, Ayaz Hassan, Graziela Cristina Sedenho, Iago A. Modenez, and Frank Crespilho

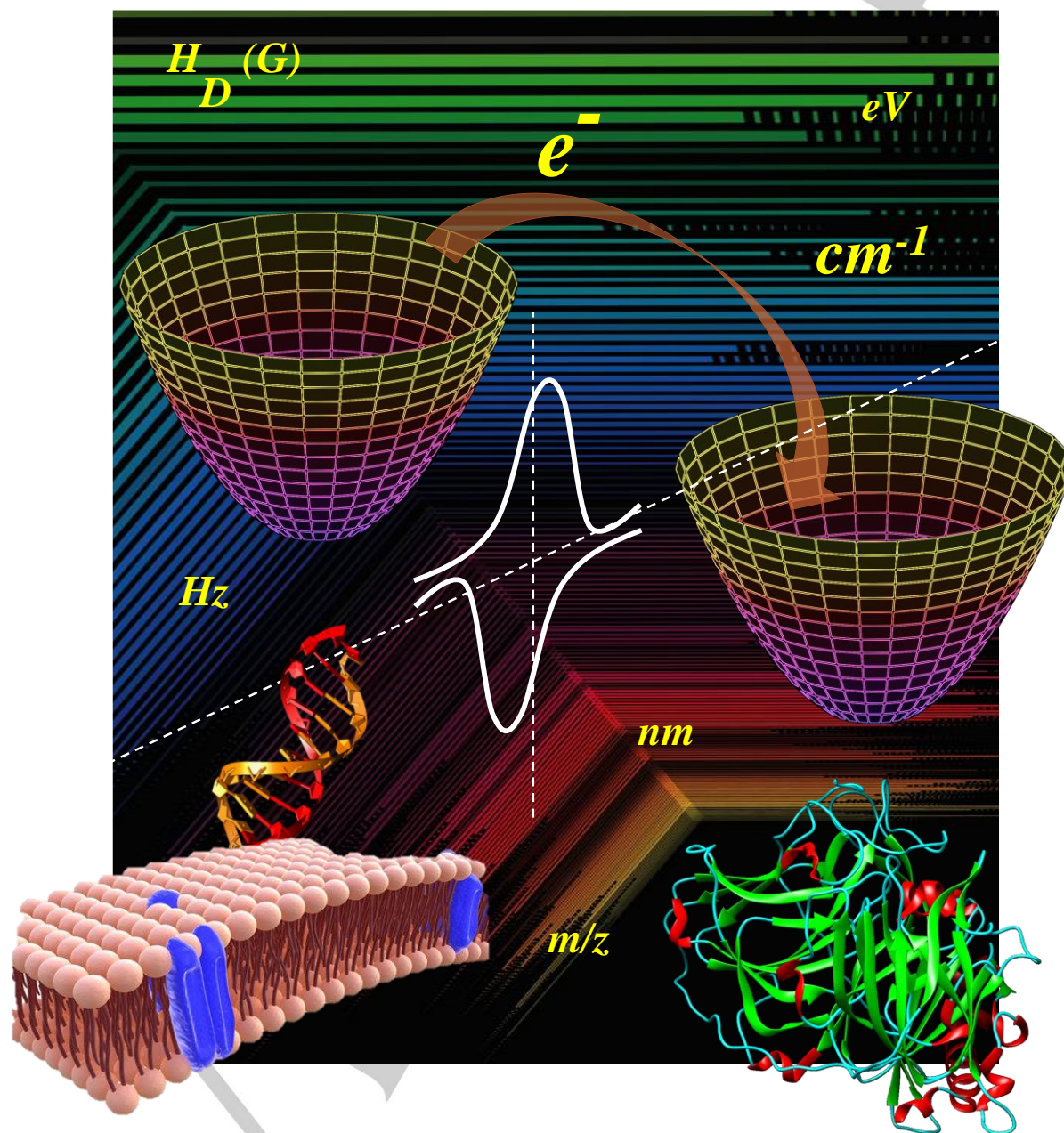
This manuscript has been accepted after peer review and appears as an Accepted Article online prior to editing, proofing, and formal publication of the final Version of Record (VoR). This work is currently citable by using the Digital Object Identifier (DOI) given below. The VoR will be published online in Early View as soon as possible and may be different to this Accepted Article as a result of editing. Readers should obtain the VoR from the journal website shown below when it is published to ensure accuracy of information. The authors are responsible for the content of this Accepted Article.

To be cited as: *ChemElectroChem* 10.1002/celc.202001327

Link to VoR: <https://doi.org/10.1002/celc.202001327>

In Situ and *Operando* Techniques for Investigating Electron Transfer in Biological Systems

João C. P. de Souza,^{[a],[b]} Lucyano J. A. Macedo,^[a] Ayaz Hassan,^[a] Graziela C. Sedenho,^[a] Iago A. Modenez,^[a] and Frank N. Crespilho^{*[a]}



- [a] Prof. Dr. J. C. P. de Souza, MS L. J. A. Macedo, Dr. A. Hassan, MS G. C. Sedenho, BS I. A. Modenez, Prof. Dr. F. N. Crespiho
São Carlos Institute of Chemistry
University of São Paulo
13560-970, São Carlos, São Paulo, Brazil
E-mail: frankcrespiho@iqsc.usp.br
- [b] Prof. Dr. J. C. P. de Souza
Campus Rio Verde
Goiano Federal Institute of Education, Science and Technology
75901-970, Rio Verde, Goiás, Brazil

Abstract: When bioelectrochemistry meets other analytical techniques for *in situ* experiments, new possibilities for understanding the nature of charge transfer reactions are provided. Despite progress in recent years in analytical instrumentation, a number of key issues remain the subject of study in bioelectrochemistry, as mechanistic description of the surface reactions involved in biomolecules' electron transfer. The main challenges of these techniques are the concomitant detection of electron transfer and molecular alteration as well as the development of suitable bioelectrodes. This review discusses the most recent and emerging *in situ* and *operando* electrochemical methods used to study biological systems such as redox proteins, nucleic acids, small biomolecules, cells, and biomembranes, focusing on electrochemical methods coupled with spectroscopic, spectrometric, and microscopic techniques.

1. Introduction

The monitoring of electron transfer (ET) in biological processes such as enzymatic redox reactions, microbial metabolite production, and DNA damage and the associated structural changes in biomolecules under the conditions of precise potential control is very insightful. In this context, *in situ* and *operando* spectroelectrochemical techniques are of key importance for obtaining in-depth information on ET pathways in biochemical processes. The coupling of electrochemistry to spectroscopic, spectrometric, and microscopic techniques is an interesting and efficient strategy of probing through-biomolecule ET processes. The combination of *in situ* and *operando* electrochemical methods simultaneously provides information on material structural organization and current flow as well as on energetic state modulation due to the application of a certain potential to molecules immobilized on or dispersed near the working electrode surface.^[1]

In situ techniques provide multi-faceted information on the structural organization of biomolecules, depending on the wavelength of the radiation interacting with the sample. Meanwhile, the term *operando* spectroscopy was carved to characterize a subgroup of *in situ* spectroscopy when this approach is used to analyze the structural changes of a system under work conditions,^[2] e.g., *in situ* measurements to visualize how raising the temperature or applying an electrochemical potential activates a catalyst and what products are obtained from this reaction. Nowadays, this term has also been extrapolated for any type of system in work regime, as it is the case of batteries.^[3]

Within the vast number of spectroscopies, some are more commonly used for *in situ* and *operando* measurements, such as Fourier transform infrared (FTIR) spectroscopy that provides information on the vibrational modes of covalent bonds within a given molecule,^[4] while X-ray absorption spectroscopy (XAS) provides information on the oxidation state of redox co-factors and their chemical environment/coordination sphere.^[5] Raman spectroscopy, another powerful vibrational spectroscopic technique, is widely used for the chemical and structural characterization of biomolecules and studies the inelastic interaction of molecules with monochromatic light, usually emitted by a laser source in the visible, near-IR, or near-ultraviolet (UV) range.^[6] Most scattered photons have the same

wavelength as incident light (Rayleigh scattering) and do not provide useful information, whereas some photons are scattered at different wavelengths (Raman scattering), which can be used to obtain useful insights. The Raman spectrum of a (bio)molecule depends on its chemical structure, conformation, redox state, etc. Raman spectroscopy has many advantages such as no need for sample pretreatment, applicability to small samples, nondestructive nature, and short analysis time. Unlike in the case of other vibrational spectroscopy techniques, water, glass, and carbon dioxide are only weakly Raman-active, which makes Raman spectroscopy attractive for spectroelectrochemical studies. However, one of the main disadvantages of Raman spectroscopy is the small Raman scattering cross-section, especially when the biological component is adsorbed at or covalently attached to an electrode surface.^[7] To overcome this limitation, surface-enhanced Raman spectroscopy (SERS) and surface-enhanced resonance Raman spectroscopy (SERRS) can be used in spectroelectrochemical studies involving biological systems.

SERS is a very selective and sensitive technique with Raman signal intensities increased by factors of up to 10^{11} .^[7] This enhancement is due to the combination of electromagnetic and chemical mechanisms in the vicinity of plasmonic nanoparticles (NPs) and/or nanostructured surfaces used as SERS substrates. The enhancement factor depends on the orientation of the adsorbed molecule and NP geometry. The traditionally used SERS substrates are Au, Ag, and Cu NPs.^[7] In this context, surface enhancement enables the spectroelectrochemical Raman studies of biomolecules immobilized on nanostructured metal electrodes.

On the other hand, electron paramagnetic resonance (EPR) spectroscopy is well suited for the identification of paramagnetic centers such as unpaired electron from free radicals. Distinctive EPR spectra are obtained for metal-containing structures, in which case the easy fluctuation between several stable oxidation states allows the existence of paramagnetic electronic configurations.^[8] EPR spectroscopy can extract site-specific information on biomolecule metal centers and their local environment by probing the free electrons in d-orbitals.^[9–11] Moreover, when coupled to electrochemical methods, this technique is well suited for elucidating the redox-active centers of biomolecules, including proteins and redox enzymes, and the associated complex redox reactions involved in the formation of EPR-detectable free radical intermediates.^[12–15] *In situ* EPR spectroscopy usually relies on two strategies, namely direct redox titration for the *in situ* generation of the active intermediate in the EPR spectroelectrochemical cell or the *ex situ* generation of paramagnetic species followed by transfer to the EPR tube for the respective measurements. The first approach is more precise, allowing the corresponding changes to be evaluated with greater control without the perturbation induced during the transfer process. In the latter case, however, the intermediates are EPR-active only at low temperatures, and redox measurements must be carried out in the frozen state, usually at liquid nitrogen temperature (77 K), which makes this approach more difficult to implement and suitable only for few molecules.^[16] EPR spectroelectrochemical experiments are particularly useful for determining the half-wave potential of redox couples when the corresponding cyclic voltammograms are very broad because of the slow ET at the electrode surface.

REVIEW

WILEY-VCH

This is mostly the case for biomolecules, as their active redox centers are deeply buried inside the molecular matrix.^[17]

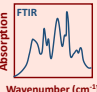
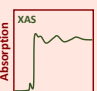
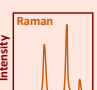
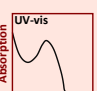
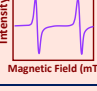
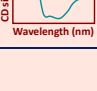
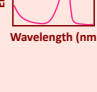
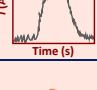

In situ Operando	Biosystem						Information	Advantages	Limitations
	Redox proteins	Redox metallic center	Nucleic acids	Small biomolecules	Biomembranes	Cells			
	✗ [43, 45]	✗ [44, 45, 46-48]					Atoms oxidation state	<ul style="list-style-type: none"> Simple, easy and fast analysis Small sample quantities required Non-destructive Relatively inexpensive 	<ul style="list-style-type: none"> Strong influence from H₂O and atmospheric CO₂ Complex mixtures give rise to complex spectra (overlapping bands)
	✗ [119]				✗ [112-114]		Structural conformation		
	✗ [37]	✗ [36, 37]			✗ [106, 116]		Catalytic reactions products/intermediates		
					✗ [112-114]		Biomembranes fusion, disruption, aggregation and hydration		
	✗ [5, 65]	✗ [54, 56-58]					Atoms oxidation state	<ul style="list-style-type: none"> Element specific Not limited to the physical state of the sample 	<ul style="list-style-type: none"> Synchrotron facility required Cryogenic conditions for most of the biological samples to minimize thermal disorder and radiation damage Moderate sample concentration
	✗ [51-53]	✗ [51-53]					Coordination sphere		
	✗ [92]						Catalytic reactions products/intermediates	<ul style="list-style-type: none"> Independent of the sample physical state No sample preparation needed No interference from H₂O Non-destructive 	<ul style="list-style-type: none"> Low sensitivity (Raman effect is weak) Laser irradiation heating may destroy the sample
			✗ [75-78]				DNA denaturation/renaturation, redox mechanism and adsorption behavior		
					✗ [91]		Biomolecule-biomembrane interactions		
							Detection and discrimination of living cells	<ul style="list-style-type: none"> Simple and inexpensive analysis High sensibility Low sample concentration needed Non-destructive 	<ul style="list-style-type: none"> Only possible with molecules with chromophore group Dependent on the sample physical state
	✗ [66]						DNA denaturation/renaturation	<ul style="list-style-type: none"> High sensibility and specificity 	<ul style="list-style-type: none"> Cryogenic conditions needed in most cases
	✗ [17]						Biomolecule-biomembrane interactions		
	✗ [86-88]	✗ [9-11]			✗ [90]		Kinetic and thermodynamic parameters		
							Atoms and coordination sphere oxidation state	<ul style="list-style-type: none"> Simple and fast analysis Relative low samples concentration Any size of macromolecule No sample preparation needed 	<ul style="list-style-type: none"> Certain buffers components can cause interference in the Far-UV Solution turbidity can cause radiation scattering influencing the determination of secondary structure
	✗ [21, 119]		✗ [74]				Redox couple half-wave potential		
							Free radical ions intermediates	<ul style="list-style-type: none"> High sensibility and specificity Insensitive to light scattering Fast response 	<ul style="list-style-type: none"> Restricted to fluorescent compounds Dependent on the sample physical state
							Structural conformation		
	✗ [125]						Biomembranes fusion, disruption, aggregation and hydration		
	✗ [18, 19]						Redox-state transitions		
	✗ [18]						Kinetic and thermodynamic parameters	<ul style="list-style-type: none"> High sensibility Fast response 	<ul style="list-style-type: none"> Only volatile products can be detected
							Intramolecular and heterogeneous electron transfer rates		
							Transport across biomembranes		
	✗ [124]						Catalytic reactions products/intermediates	<ul style="list-style-type: none"> No sample preparation needed Does not require vacuum or controlled atmosphere It is not limited to dried samples, works in solid-liquid interfaces Spatial resolution Three-dimension surface profile 	<ul style="list-style-type: none"> Limited vertical and magnification ranges Low scanning speed Tip or sample can be damaged
	✗ [24]						Kinetic and thermodynamic parameters		
							Biomolecules mapping/distribution on electrode surface or inside living cells		
							Identification and structural characterization of membranes/cells		
							Cellular homeostasis and cytomembranes permeability		

Figure 1. Operando and *in situ* techniques applied for bioelectrochemistry studies.

Spectroelectrochemical techniques based on fluorescence and UV-visible (UV-vis) absorption spectroscopy allow one to assess the thermodynamic and kinetic parameters of bioelectrochemical systems,^[18–20] while circular dichroism (CD) spectroscopy traditionally provides structural information (e.g., the secondary structure of proteins and DNA denaturation) on biomolecules.^[21] Fluorescence is an optical phenomenon based on the excitation of a ground-state molecule through the absorption of photons with a specific wavelength. After excitation, the absorbed energy may be released through several photophysical events such as the emission of a photon with another wavelength, which forms the basis of fluorescence. Fluorescence spectroscopy is widely used for the detection of biomolecules and is commonly employed in biological and biomedical applications because of its high spatial and temporal resolution.^[20] In addition, when coupled to electrochemical methods, fluorescence spectroscopy can provide information on the redox-state transitions of biomolecules and distinguish between intramolecular and heterogeneous ET because of the change in emission intensity with the change in redox state. Biomolecule-membrane interactions, for example, can be probed in different ways by modifying the environment of a fluorescent probe, which can furnish information on lipid membrane disruption, fusion, or aggregation. Aromatic amino acids in proteins, such as tryptophan and tyrosine, can also be probed by *in situ* fluorescence spectroscopy to obtain information on their position, orientation, and insertion into biological membranes.^[23]

A new *operando* technique not involving electromagnetic radiation has been developed for enzymatic activity monitoring by combining electrochemical control with mass spectrometry.^[22] The corresponding setup features a combination of an electrochemical cell with a mass spectrometer, and the technique itself is known as *operando* differential electrochemical mass spectrometry (DEMS). The main advantage of DEMS is its suitability for the online detection of volatile and gaseous compounds under the conditions of precise potential control.^[24]

The coupling of electrochemical methods to microscopic techniques is an interesting approach, especially when higher spatial distribution is required or only a microscopic and specific area of the electrode surface or few molecules should be characterized. Among the microscopic techniques, atomic force microscopy (AFM), scanning tunneling microscopy (STM), confocal microscopy, fluorescence microscopy, and optical microscopy have been extensively and successfully coupled to electrochemical methods for the *in situ* mapping of biomolecules or drug distribution on the electrode surface or inside cells, sensing interaction forces, or structural/chemical imaging under the conditions of electrochemical control.

The development of *in situ* and *operando* electrochemical techniques applicable to biosystems is challenged by the structural and chemical complexity of these systems,^[25] the need to keep biological entities dispersed or immobilized on the working electrode,^[26] and the requirement to obtain an optimal setup for bioelectrochemical cells. Herein, we review the most recent advances (especially those of the last five years) in *operando* and *in situ* electrochemical methods applied in the studies of biosystems and the related prospects for the elucidation of the redox reaction mechanisms of biological entities. This review is divided according to the five main classes of biological systems that can be investigated by *in situ* and *operando* spectroelectrochemistry, namely redox proteins, nucleic acids, small biomolecules, cells, and biomembranes (Figure 1).

Prof. Dr. João C. Perbone de Souza received his BS in chemistry from the Federal University of Alfenas (Brazil) in 2013 and obtained a PhD in physical chemistry in 2017 from the São Paulo University (Brazil) under the supervision of Prof. Frank N. Crespilho. During his PhD, Prof. de Souza developed a new approach to the investigation of enzymatic kinetics using differential electrochemical mass spectrometry. Currently, he is a Professor at the Goiano Federal Institute of Education, Science and Technology (Brazil).



Lucyano J. A. Macedo received his BS in chemistry from the Federal University of Piauí, Brazil (2016) and obtained his MS in physical chemistry from the University of São Paulo, Brazil (2018). He was a visiting researcher at the University of Wisconsin-La Crosse, USA (2014–2015) and is currently a PhD candidate in physical chemistry at the University of São Paulo. His research interests focus on electron transfer processes within metalloenzymes containing Cu and Fe centers.



Dr. Ayaz Hassan received his BS in chemistry from the University of Peshawar (Pakistan) in 2005 and obtained his MS in chemistry from the same university in 2007, further graduating with a PhD in chemistry from the Institute of Chemistry of São Carlos, University of São Paulo (Brazil) in 2015. Currently, he is a postdoctoral researcher in the same institute, working with Prof. Frank N. Crespilho and mainly focusing on *in situ* FTIR spectromicroscopy and the development of monolayer graphene-based biosensors and biodevices.



Graziela C. Sedenho received her BS in technological chemistry (2013) and an MS in chemistry (2016) from the São Paulo State University (UNESP), Brazil and is currently a PhD student at the University of São Paulo (USP), Brazil. She was a visiting researcher at the University of Oxford (2014–2015) and at the Harvard University (2018–2019), currently focusing on electrochemistry, electron transfer mechanisms involving redox proteins and microorganisms, electrode materials, and electrochemical systems for energy conversion and storage.



REVIEW

WILEY-VCH

Iago A. Modenez received his BS in technological chemistry from the Federal University of São Carlos (UFSCar), Brazil (2018), and is currently an MS student in physical chemistry at the University of São Paulo (USP), Brazil. His research focuses on metalloproteins and biological electron transfer mimicry using nanostructured inorganic materials and cellular model membranes.



Frank N. Crespilho is professor of physical chemistry at the São Carlos Institute of Chemistry, University of São Paulo (USP), deputy coordinator at the Institute of Advanced Studies (IEA-USP, São Carlos), and fellow associate at Harvard University (2018–current). He was a visiting associate in chemistry at Caltech USA (2014–2015) and at the Max Planck Institute for Solid State Research in Stuttgart (2016). His research focuses on fundamental and applied aspects of biomolecule redox chemistry, electron transfer, and *in situ* and *operando* spectroelectrochemistry.



2. ET and heterogeneous enzyme catalysis

Redox proteins play a crucial role in many important biological processes that involve ET or redox reactions, e.g., photosynthesis, respiration, metabolism, nitrogen fixation, molecular signaling, and cell apoptosis. The core of redox proteins corresponds to redox centers that drive the thermodynamics and kinetics of ET during enzymatic reactions and typically feature non-amino-acid functional groups. These functional groups can be either metal ions, which are very tightly or even covalently bound to protein matrices (cofactors) or organic molecules/organometallic transient carriers (coenzymes). Thus, according to their redox centers, redox proteins can be divided into metalloproteins, flavoproteins, quinoproteins, and nicotinoproteins.

The processes involved in redox protein operation can be investigated using *operando* electrochemistry. The combination of FTIR with electrochemistry for the assessment of reactions involving proteins and the mechanistic investigation of redox enzyme-promoted reactions offers a versatile analytical tool for obtaining time-resolved information up to a short time scale, from ps to ms. This technique allows light and redox potential to be simultaneously used as triggers to follow the structural changes in the functionality of active sites as functions of the electrode potential.^[27–30] The above method can also be used to probe changes in the protein secondary structure, the amino acid side chain (because of localized protonation), and the coordination at the metal cofactors of metalloproteins.^[21–33] However, for the successful implementation of this technique, one should be able to measure the absorption signal of some vibrational marker of the protein monolayer adsorbed on the finite area of the electrode surface with a protein concentration of the order of $\mu\text{mol cm}^{-2}$.^[33,35]

The intense background signal of the bulk phase limits the detectable signal of redox reaction-induced vibrational changes of proteins to far less than 1% of the absolute intensity. Additionally, *in situ* FTIR measurements in aqueous electrolytes impose further restrictions on the experimental setup, as water has a high molar absorptivity in the mid-IR region and strongly interferes with the sample absorption signal.^[4] Several strategies have been adopted to develop *in situ* methods, employing different designs of the experimental setup and the electrochemical cell to keep the amount of water in the path as low as possible and enhance the absorption signal of adsorbed molecules.^[36–38] This technique can be implemented in both transmission and reflection modes in the mid-IR regions; however, *in situ* measurements in transmission mode are somewhat uncommon because of the large background signal from the aqueous electrolyte. On the other hand, approaches using the reflection mode have been more successful because of the excellent electrochemical control achieved upon coupling to electrochemistry and can be used either in IR reflection absorption (IRRA) or attenuated total reflection (ATR) FTIR spectroscopy. Thus, several studies have combined these techniques with electrochemistry.^[39,40]

ATR FTIR spectroscopy relies on the internal reflection of IR light, and the electrochemical cell is preferentially constructed on the top of the ATR prism, in which case the working electrode geometry can be easily optimized for a fast response of the applied potential. One such example is protein film infrared electrochemistry (PFIRE), which employs a redox enzyme-modified carbon electrode placed on the ATR prism. As redox enzymes can be easily immobilized on carbon surfaces, *in situ* electrochemical measurements can be performed with easy control during enzyme-catalyzed reactions.^[41]

Surface-enhanced infrared absorption (SEIRA) spectroscopy is based on the enhancement of the absorption signal of a protein film on a metal surface and can even be performed using the direct deposition of a thin metallic film on the ATR prism, which is then used as the working electrode.^[42] This method is very sensitive to molecules adsorbed on the electrode surface, not only minimizing the interference of water, but also allowing one to monitor the spectral changes at the submonolayer of the adsorbed protein due to the enhancement of the signal by several orders of magnitude. Several membrane proteins have been investigated to elucidate their structure and understand the mechanism of ET at the electrochemical interfaces in adsorbed states. For example, the potential of sensory rhodopsin II was electrochemically controlled by using SEIRA spectroscopy of this membrane protein immobilized on Au as a self-assembled monolayer.^[43]

FTIR difference spectra were recorded simultaneously with the application of a potential to the protein-modified Au working electrode against the reference and counter electrodes. As the potential increased to >0.2 V, the band corresponding to the C=O stretching vibration ($\nu_{\text{C=O}}$) at 1764 cm^{-1} retained its intensity (Figure 2A) but broadened, which was attributed to the impact of the applied electric field on this band and the associated hydrogen bonding network. In contrast, a decrease in the applied potential caused the band to almost disappear at -0.3 V, as proton transfer from the Schiff base (retinal) to the carboxylic acid side chain of the D75 residue (Asp75) becomes difficult at negative potentials because of the concomitant increase in the corresponding energy barrier. The energy induced by this negative potential is insufficient to overcome this barrier. Indeed, at negative potentials, the dissociation of the Schiff base proton is forced toward the cytoplasmic side (Figure

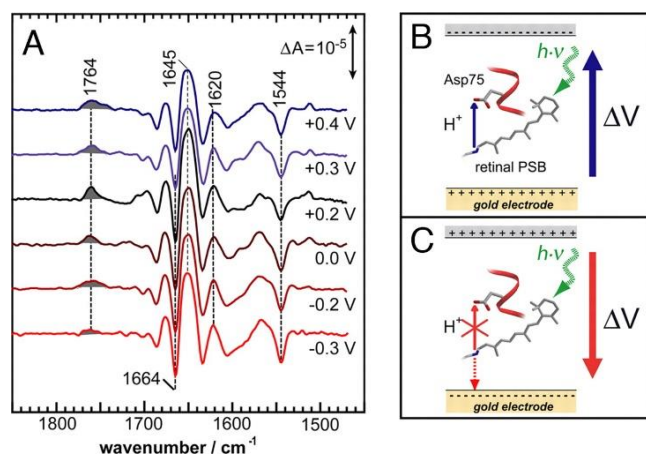


Figure 2. SEIRA spectra recorded at various transmembrane voltages across the membrane protein monolayer. (A) IR difference spectra of sensory rhodopsin II from *N. pharaonis* were recorded at potentials from +0.4 V to −0.3 V vs. the normal hydrogen electrode (top to bottom). (B) Sketch of light-induced proton transfer (thin blue arrow) from the donating retinal Schiff base of sensory rhodopsin II to the accepting carboxylic side chain of D75. The proton transfer step occurs in the direction of the electric field vector (thick blue arrow indicating the transmembrane voltage ΔV between the working Au electrode (+) and the counter electrode (−)). (C) Protonation of D75 ceases (crossed out red upward arrow) when ΔV is applied in the opposite direction (bold red arrow) and is lower than −0.2 V. In this case, the negative voltage drives the Schiff base proton toward the cytoplasmic side (red downward arrow). Reprinted with permission from Ref. 43, Copyright (2008) National Academy of Sciences, U.S.A..

2C). FTIR spectroscopy plays an important role in elucidating the ET mechanisms of hydrogenases, as these enzymes feature organometallic cofactors. The coordination sphere of these cofactors features iron ions coordinated to cyanide (CN[−]) and carbonyl (CO) ligands, which exhibit high-molar-absorptivity stretching vibrational modes beneficial for FTIR spectroscopic analysis. Moreover, the window in which these groups absorb radiation is free from the interference of water, which is usually used to dissolve proteins and the supporting electrolyte.

As ligand vibrational modes are sensitive to the oxidation state of the metal center they are coordinated to (Figure 3A), the evolution of these bands provides valuable mechanistic insights. Because of their high catalytic activity, hydrogenases usually produce high catalytic currents and have been extensively investigated by *in situ* FTIR spectroscopy coupled with protein film voltammetry. One such example is the elucidation of the mechanism of redox communication between the metal-containing prosthetic groups in a [FeFe] hydrogenase from *Chlamydomonas reinhardtii*.^[44] The changes in the infrared signature for the redox reaction of each cluster, which reflect the changes in the redox behavior of the H-cluster responsible for the docking and further reduction of protons (Figure 3B), revealed that inter-cluster communication enhanced proton-coupled electronic rearrangement in the H-cluster, which is associated with efficient H₂ production even at high pH. Vincent et al. used PFIRE (Fig. 3C)^[37] to demonstrate the formation of intermediates such as Ni_a-R and Ni_a-C (which are common to all [NiFe] hydrogenases) during catalytic turnover. The FTIR spectra of *Escherichia coli* Hyd-1 were recorded under catalytic and non-catalytic conditions at two different applied potentials vs. the standard hydrogen electrode. At a negative applied potential (−0.074 V), the spectra recorded in the presence of Ar (non-catalytic condition) exhibited bands corresponding to Ni_a-SI (green) and Ni-B (blue, inactive state) states, while only one state (Ni-B) was observed at +0.356 V.

However, in the presence of H₂ (catalytic condition), two new states of Ni_a-R (red) evolved, and the content of the Ni_a-SI state decreased (Figure 3D). The difference between the non-catalytic and catalytic conditions became obvious at +0.356 V, when Ni_a-SI, Ni_a-C, Ni_a-R, and Ni_a-L (orange) appeared in the presence of H₂, in contrast to the results obtained under non-catalytic conditions (Ar). The time-independent current observed during catalytic turnover suggested the occurrence of efficient mass transport on the surface of the hydrogenase-grafted electrode, whereas a monotonic decrease in current was observed at +0.356 V because of the oxidation-induced conversion of the enzyme into the inactive Ni-B state.

In situ FTIR spectroelectrochemistry provides insightful information on the activity of nitrogenases, which mostly promote the reduction of N₂ (inert under physiological conditions) to more reactive nitrogenated species such as ammonia. However, as this reaction competes with proton reduction to H₂, the nitrogenase cofactor has been studied to understand the mechanism of switching between proton/nitrogen reduction and elucidate how the organometallic moiety of these enzymes can be modulated to such a role by observing the behavior of induced CO ligands in the FeMoCO-cluster.^[36] This approach has also been used to probe the effect of inhibitors on internal ET in other enzymes. Similarly to CN[−] and CO, azide (N₃[−]) is a useful ligand for probing the oxidation state of the metal it is coordinated to. A study using multicopper oxidases investigated the inhibitory effects of fluoride and chloride on the performance of laccase and bilirubin oxidase in the oxygen reduction reaction. Signals inherent to the N≡N moiety of this ligand coordinated to the Cu centers of the prosthetic group showed that the size of the inhibitor allows it to bind to different enzyme sites. For instance, as a small ion, fluoride can access the trinuclear cluster responsible for oxygen reduction and thus directly inhibits oxygen binding. Meanwhile, the larger chloride ion cannot access this site and binds to the type 1 Cu center and inhibits oxygen reduction by limiting the internal ET from this center to the trinuclear one.^[45]

In situ FTIR spectroscopy, which can be applied in the region below 400 cm^{−1} (far infrared), is complementary to Raman spectroscopy and is sometimes used to monitor the redox reaction-induced changes of metal-ligand bond vibrations in the vibrational spectroscopic studies of proteins. Instead of indirectly correlating ligand behavior to the metal in the coordination center, several research groups have used the above technique to directly probe the behavior of the metal center and its surrounding ligands in metalloproteins. Far-infrared radiation induces the vibrations of bonds involving heavy atoms such as transition metals, which can be used to obtain the spectral signatures of certain vibrational modes correlated to the redox activity of metalloenzymes with interactions such as Fe–S, Fe–N, and Cu–S.^[46–48] The limited use of this approach to unveil metalloenzymatic reaction mechanisms is due to the difficulty of obtaining reasonable signal-to-noise ratios. The mechanism of metalloenzyme operation can also be investigated by *operando* electronic absorption or emission (XAS, fluorescence, and UV-vis) spectroscopy. Among these techniques, XAS allows access to individual elements, as the energy window required for the excitation and further transition of internal shell electrons is atom-specific, and thus provides unambiguous electronic and geometric information at the atomic level.^[49,50] This technique has taken precedence over several other spectroscopic techniques, as the large penetration depth of high-energy X-rays enables *in situ* measurements under ambient conditions. In this way, one can obtain molecular-level information on the species present in very dilute solutions (μM to mM), and the above method is therefore ideal for probing the oxidation states of metal centers and their chemical environment in biological systems.^[51–53] Sometimes, this technique is the only method of studying spectroscopically silent metal cofactors such as Cu(I)

REVIEW

and Zn(II)^[54] and allows the indirect detection of biologically relevant nonmetallic elements (such as S) whose XAS edge is very sensitive to oxidation state changes and experiences a significant alteration of signal intensity in response to these changes.^[55] When used as a standalone technique in non-electrode *ex situ* redox experiments, XAS provides important information on the electronic behavior of (mostly) metals and supplies insights into the biological role of such metal-containing structures.^[56–58] However, the evaluation of ligand structure around coordination centers is very important to uncover their role in biological activity and biomimetic systems biocatalyzed by proteins and enzymes. Such information can only be obtained by combining *in situ* XAS with electrochemistry. Several groups have used *operando* XAS in electrochemical systems to pursue goals ranging from studying the electrochemical activity and stability of electrocatalysts under oxygen reduction reaction (ORR)^[59] and oxygen evolution reaction^[60] conditions to studies of charge/discharge in Li-ion batteries,^[61] and some excellent reviews on this topic have been published.^[62–64] However, surprisingly few reports have dealt with the use of *operando* XAS analysis in bioelectrocatalysis under the conditions of electrochemical potential control. Fe-, Zn-, and Cu-containing biomolecules are most widely studied by XAS; hence, earlier studies in this direction have dealt with multicopper oxidases, which contain at least four Cu centers and are excellent bioelectrocatalysts for the ORR at physiological pH and temperature. The Cu K-edge X-ray absorption spectra of the different states of laccase

obtained through *ex situ* chemical reduction indicated the presence of reduced (Cu^+), fully oxidized (Cu^{2+}), and intermediate states of the enzyme under turnover conditions in the presence of O_2 .^[65] In agreement with the results of other spectroscopic techniques, the slow decay of the intermediate native state to the resting state (Cu^{2+}) was attributed to changes in the trinuclear Cu center, which allows for efficient ET during the catalytic process. Similarly, the bioelectrochemical behavior of bilirubin oxidase from *Myrothecium verrucaria* (MbOD) was evaluated under catalytic and non-catalytic conditions using *operando* XAS (Figure 4A–D).^[3] Figure 4E shows the Cu K-edge X-ray absorption spectra of MbOD recorded at different electrochemical potentials, illustrating the evolution of a redox reaction. This reaction comprised the reduction of Cu^{2+} , as revealed by the attenuation of the signal at 8997 eV and the concomitant rise of the signal at 8983 eV owing to the presence of Cu^+ in the enzymatic structure. Compared to the case when O_2 is absent in the bioelectrochemical system, the bonding of O_2 to the trinuclear cluster results in a 150-mV increase of the onset potential in the potentiometric titration curve (Figure 4F) in the presence of Cu^+ . This behavior suggests the occurrence of fast ET from T1 to the trinuclear cluster and the ability of the metal cofactor to act as an electronic bridge connecting the electron donor (organic substrate or electrode surface) and the electron acceptor (O_2) in two distant parts of the enzyme for a faster and more energetically favorable ET.

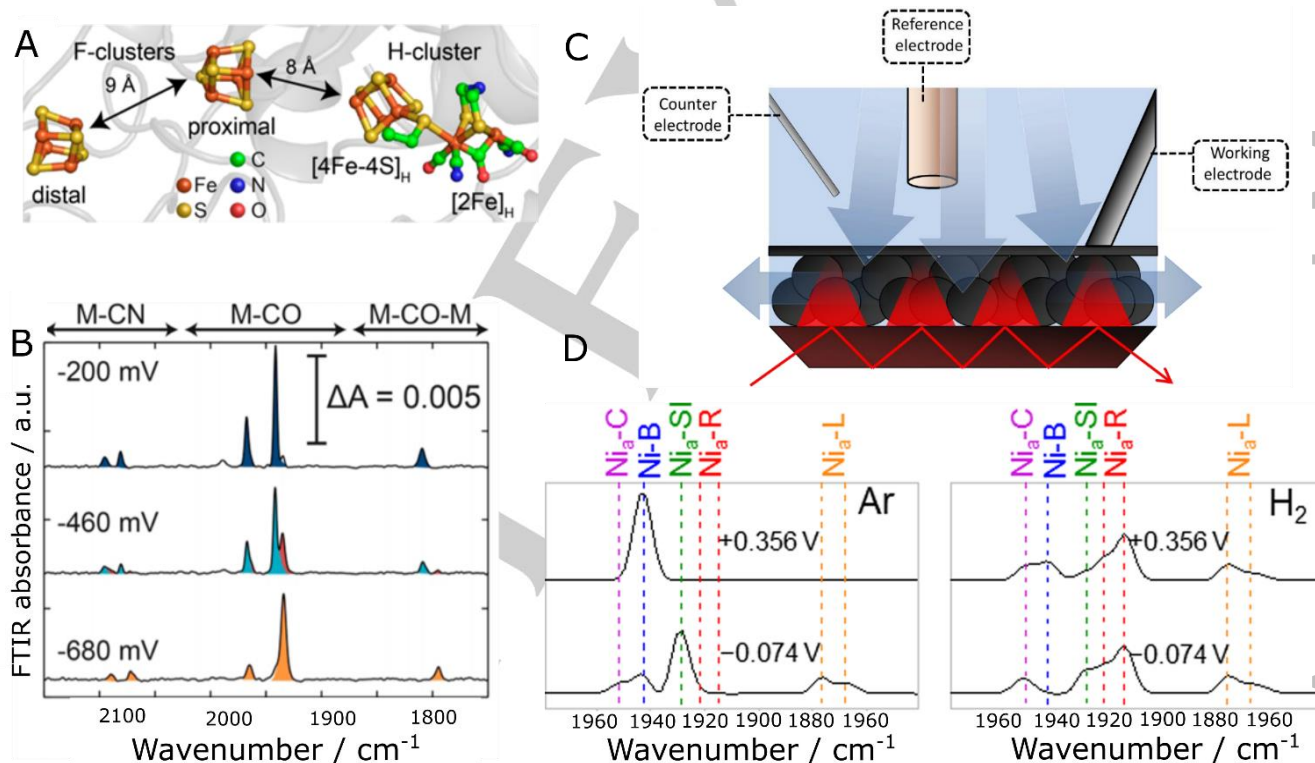


Figure 3. (A) Structure and spatial distribution of metal clusters within [FeFe] hydrogenase from *C. reinhardtii*. (B) FTIR spectroelectrochemical response of ligands in the cofactors. (C) Schematics of the spectroelectrochemical ATR-IR cell designed for PFIRE experiments showing the relative location of electrodes and the direction of solution flow. (D) IR spectra of *E. coli* Hyd-1 recorded using the PFIRE technique under non-turnover (Ar, left panel) and steady-state electrocatalytic turnover (H_2 , right panel) conditions. These spectra reveal the states formed in response to electrocatalytic H_2 oxidation. Panels A and B are reprinted with permission from Ref. 44. Panels C and D are reprinted with permission from Ref. 37.

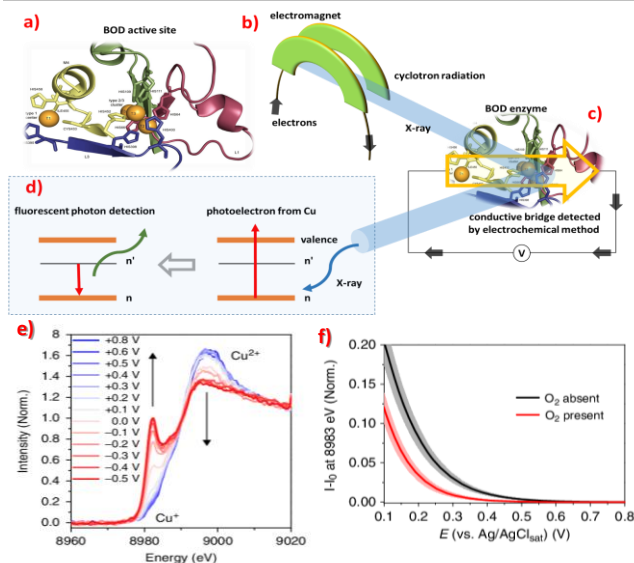


Figure 4. Assessment of ET reactions and catalysis in multicopper oxidases using *operando* XAS. (A) Representation of the crystal structure of MbOD (PDB: 2XLL) zoomed in at the four Cu ions. (B) Schematics of synchrotron radiation generation. The XAFS2 beamline of the Brazilian Synchrotron Light Laboratory (LNLS), a national institution responsible for operating the only synchrotron light source in Latin America, was used. (C) Principle of XAS spectroelectrochemical analysis. (D) Simplified scheme showing the fundamental processes required to obtain *in situ* XANES spectra during bioelectrochemical characterization, with X-ray photoabsorption of core-level electrons followed by photoelectron emission and fluorescence. (E) Potentiometric curves of Cu^+ signal intensity under each atmospheric condition highlighting the rise of this signal at different overpotentials. (F) Schematic mechanism of internal ET in the presence of O_2 bonded to the active site of MbOD. Reprinted from Ref. 5 with permission from the Nature Publishing Group, 2020.

Fluorescence spectroscopy combined with electrochemical methods provides information on the intramolecular and interfacial ET rate of nitrite reductase (NiR) from *Alcaligenes faecalis* S-6,^[18] allowing the assessment of thermodynamic and kinetic parameters. This technique, called FluRedox, provides a more direct proof of the NiR catalytic cycle. NiR has a homotrimeric structure; therefore, the distances of the three redox sites to the electrode surface are different, which affects the heterogeneous interfacial ET kinetics. Intramolecular ET is affected only by substrate concentration, and hence, the use of high concentrations at lower pH inhibits NiR. A similar approach was used to study azurin from *Pseudomonas aeruginosa* with a single Cu ion as the redox-active center, revealing that the orientation of the enzyme on the electrode surface influences the rate constant of ET.^[19] This experiment was carried out using a transparent Au electrode with an immobilized enzyme to obtain electrochemical parameters, and fluorescence intensity was measured using a fluorescence microscope.

The UV-vis spectroelectrochemical approach was used to investigate the ET of *Schizosaccharomyces pombe* ferredoxin and the influence of substitution of some amino acid residues in the protein structure.^[20] In this study, an in-house-made optically transparent thin-layer electrochemical cell was used, and an Au minigrad was employed as the working electrode.

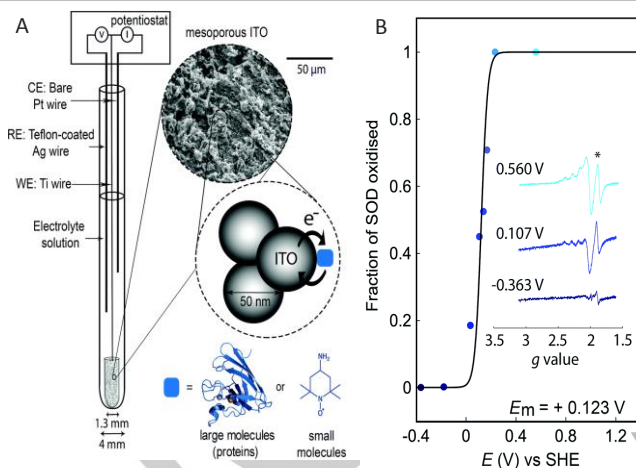


Figure 5. EPR spectroelectrochemical response of superoxide dismutase (SOD) in the PFE-EPR cell. (A) Schematic diagram of the PFE-EPR spectroelectrochemical cell. (B) Intensity of the g_{xy} transition of Cu^{2+} in SOD (dots) vs. applied potential and the corresponding fit (solid line). Inset: CW EPR spectra (16 K) of surface-bound SOD. *Signal from meso-ITO electrode. Reprinted with permission from Ref. 66.

The substitution of cysteines for serines at the active site did not affect binding affinity but decreased ET efficiency. Moreover, this substitution altered the electronic structure of the active site cluster, and the activation barrier for electron exchange increased rather than the directional coupling of any specific cysteine to the cluster.

Operando magnetic spectroscopy is also used to study the mechanisms of redox enzyme operation. Protein film voltammetry in combination with EPR (PFV-EPR) spectroscopy (Fig. 5A) was used to study a Cu-Zn superoxide dismutase-modified meso-ITO electrode. As the potential was swept from ~ 0.8 to ~ 0.4 V vs. the standard hydrogen electrode, the EPR signal intensity decreased because of the conversion of Cu^{2+} to Cu^+ , the active redox center of the enzyme.^[66] The redox potential calculated from the plot of EPR g_{xy} transition intensity vs. applied potential (Nernst curve, Figure 5B) was in good agreement with that calculated from the corresponding cyclic voltammogram, which demonstrated the promise of this technique for the precise control of the electrochemical potential of biomolecules.

DEMS, a mass-spectrometric *operando* technique, was used to study ethanol oxidation by alcohol dehydrogenase (ADH).^[24] The two products of this enzymatic reaction (NADH and acetaldehyde) were detected using electrochemical and mass-spectrometric techniques, as schematically shown in Figure 6A. NADH can be detected by electro-oxidation at the electrode surface, as this oxidation generates a time-dependent faradaic current. To enhance this current, the electrodes were physicochemically treated to produce quinone-like groups at the electrode surface, which are well-known electrocatalysts for NADH electro-oxidation. Acetaldehyde production was detected by mass-spectrometric monitoring of the mass/charge ratio (m/z) of molecular ions and related fragments. In the bioelectrochemical evaluation of ethanol oxidation by ADH, ions with m/z 29 and 22 were detected, corresponding to the main fragment of acetaldehyde (COH^+) and doubly charged carbon dioxide (CO_2^{2+}), respectively.

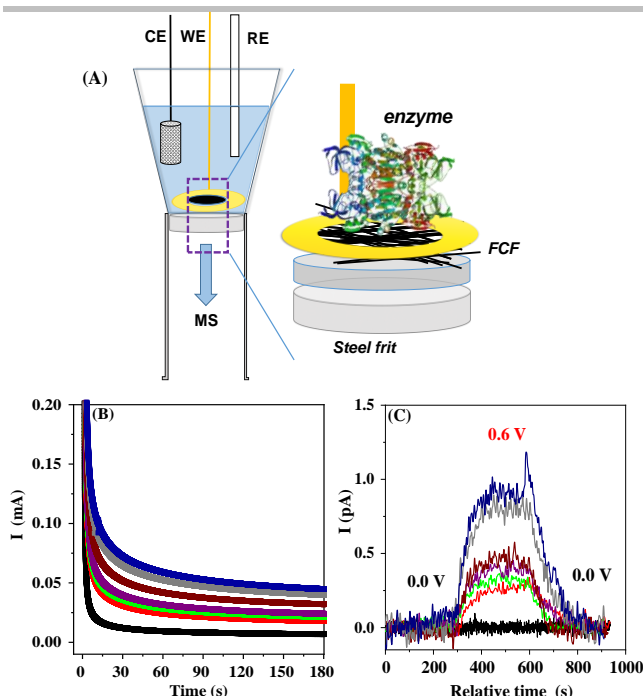


Figure 6. (A) DEMS setup showing the electrochemical cell, where CE stands for the counter-electrode, WE stands for the working electrode, the black region denotes flexible carbon fiber with immobilized ADH, the yellow region is a Au electrical connection, and RE is the reference electrode ($\text{Ag}/\text{AgCl}/\text{Cl}^-_{\text{sat}}$). The interface comprises a polytetrafluoroethylene membrane covering a steel frit. (B) Chronoamperograms at 0.6 V vs. $\text{Ag}/\text{AgCl}/\text{Cl}^-_{\text{sat}}$ of FCF-ADH recorded in the DEMS experiment for ethanol concentrations of up to 0.8 mol L^{-1} . (C) Mass intensity peak monitoring at $m/z = 29$ and 22 upon the application of overpotentials of 0.6 V and 0.0 V (vs. $\text{Ag}/\text{AgCl}/\text{Cl}^-_{\text{sat}}$), each line represents an MS chronoamperogram. Adapted from Ref. 24.

Figure 6B shows the chronoamperograms of the faradaic current obtained during the polarization of the ADH bioelectrode at 0.6 V vs. $\text{Ag}/\text{AgCl}/\text{Cl}^-_{\text{sat}}$, revealing an increase in current with increasing ethanol concentration. Figure 6C presents the chronoamperograms of ionic current for m/z 29 and 22. The ADH bioelectrode was polarized at 0.0 and 0.6 V vs. $\text{Ag}/\text{AgCl}/\text{Cl}^-_{\text{sat}}$ at different times. The black line corresponds to the ionic current of m/z 22 (CO_2^{2+}) and was used as the background, as no CO_2^{2+} production was expected. The other lines correspond to the ionic current of m/z 29 (COH^+), showing that this current increased when the electrode was polarized at 0.6 V vs. $\text{Ag}/\text{AgCl}/\text{Cl}^-_{\text{sat}}$ and was proportional to the concentration of ethanol in the electrolyte. The data of faradaic and ionic currents were used to calculate the enzymatic kinetic parameters from the Michaelis-Menten model, e.g., K_M/V_{max} was determined from the double-reciprocal plot.^[24]

3. DNA, RNA, and conformational changes

Nucleic acids play important roles in a wide range of essential cellular processes such as cellular reproduction and protein biosynthesis.^[67] Depending on the content of purines or pyrimidines and the environment, DNA adopts several conformations. Moreover, DNA structure can be altered during physicochemical processes such as hybridization and denaturation.^[68] DNA replication is a crucial biological process that involves the reversible interconversion between double-stranded DNA (dsDNA) and single-stranded DNA (ssDNA)^[69] and relies on the breakage/formation of new intermolecular

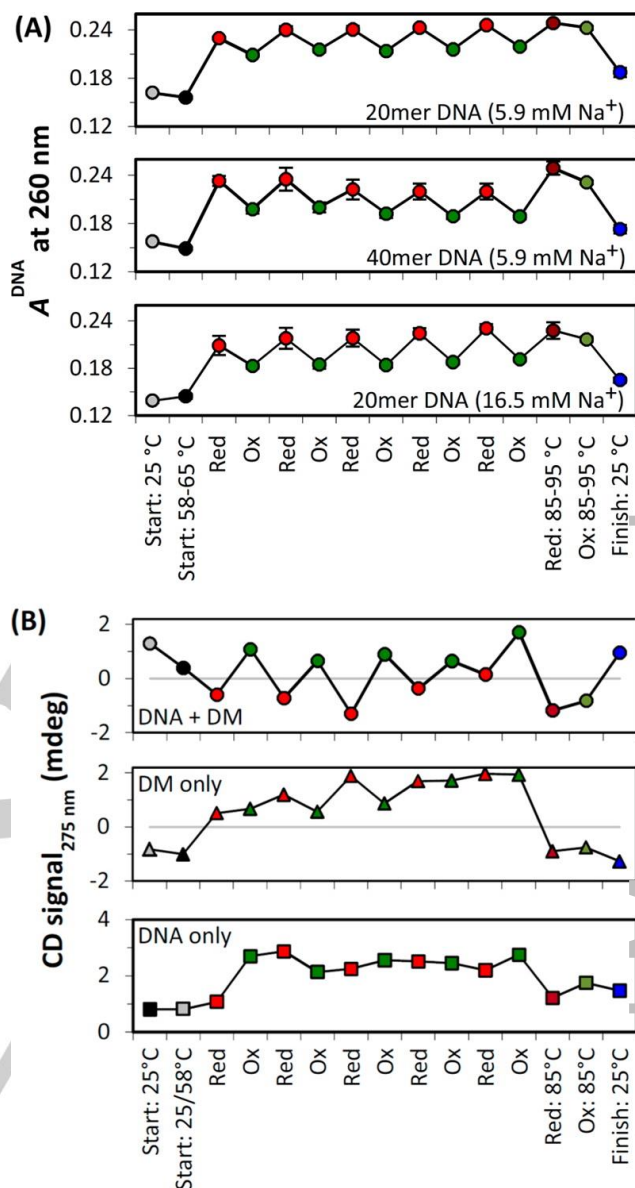


Figure 7. (A) Switch diagrams displaying the change in absorption at 260 nm due to five consecutive cycles (144 s/cycle) of DNA denaturation (red circles) and renaturation (green circles) controlled by switching the DM redox state at three different experimental conditions. Signals represent the exclusive absorbance of DNA under the given conditions. (B) Validation of electrochemically controlled DNA denaturation and renaturation cycles by *in situ* CD spectroelectrochemistry. Switch diagram of the change in $\text{CD}_{275 \text{ nm}}$ for dsDNA in the presence of DM and controls (DM only and dsDNA only). Consistent switching upon cycling between -0.8 and $+0.3 \text{ V}$ was only seen for DNA in the presence of DM. Adapted from Ref. 74.

bonds such as hydrogen bonds, π - π stacking interactions, and van der Waals interactions.^[70] The denaturation/renaturation of dsDNA can be controlled by changing temperature,^[71] pH,^[72] and ionic strength.^[73]

The cyclic denaturation and renaturation of dsDNA was studied by *in situ* UV-vis and CD spectroelectrochemistry.^[74] A representative study used an electroactive ds-DNA intercalator, daunomycin (DM), which works as an electrochemical trigger. When DM is reduced by application of an electrochemical potential, the thermodynamic stability of dsDNA decreases, and the double helix dissociates into single strands. DM can be

REVIEW

WILEY-VCH

reoxidized to promote single-strand renaturation. An *in situ* UV-vis spectroelectrochemical setup was used to measure radiation absorption upon electrochemical cycling and promote the de- and renaturation of DNA oligonucleotides. The reversible interconversion between dsDNA and ssDNA was achieved by electrochemical cycling between DM redox states upon switching the potential from -0.8 to $+0.3$ V at a working temperature of 58 °C. *In situ* UV-vis spectroelectrochemistry allowed one to monitor the behaviors of DNA and DM simultaneously. Changes in DNA conformational states upon potential switching were monitored at 260 nm, whereas intercalation and DM redox state changes were monitored at 400 – 500 nm. Figure 7A shows the results of monitoring DNA de- and renaturation by UV-vis spectroelectrochemistry (at 260 nm) under three different experimental conditions upon potential switching, while Figure 7B presents the results obtained when this monitoring was carried out using CD spectroelectrochemistry (detection wavelength = 275 nm).^[74]

Electrochemical SERS (EC-SERS) is a versatile technique for DNA analysis used to investigate ds-DNA dehybridization, redox mechanisms, and adsorption behaviors of DNA bases. For example, EC-SERS has been employed for the detection of disease biomarkers in the development of a sensor for tuberculosis diagnosis.^[75] In this case, screen-printed electrodes modified with Ag nanoparticles (AgNPs) were used as an aptasensor platform onto which the target DNA-specific aptamer was adsorbed. Direct detection of the target tuberculosis DNA was performed through the observation of characteristic SERS peaks present only in the target strand. Modulation of the applied potential allowed for a sizable increase in the observed SERS response.

EC-SERS has also been used to study the mechanism of purine base oxidation, differentiating the oxidation intermediates and their orientation during the different oxidation steps on Au nanoparticles at different electrode potentials.^[76] In this case, EC-SERS allowed not only the characterization of adenine and guanine oxidations, but also provided information on the orientation of each intermediate on the metal surface.

Additionally, *in situ* SERS measurements allow for the fast and efficient (on the timescale of minutes) detection of single nucleotide polymorphism based on potential-assisted dehybridization of target dsDNA.^[77]

Shell-isolated nanoparticle-enhanced Raman spectroscopy (EC-SHINERS) is another emerging vibrational spectroscopic method with great potential for the *in situ* analysis of biomolecules at electrochemical interfaces with a well-defined substrate. For example, EC-SHINERS was used to investigate the adsorption behaviors of adenine, guanine, thymine, and cytosine on atomically flat Au single-crystal electrode surfaces.^[78] The spectroscopic results obtained for these DNA bases revealed similar features such as the adsorption-induced reconstruction of the Au(111) surface and the drastic Raman intensity reduction of ring breathing modes after the lifting reconstruction.

Most studies investigating the mechanisms of the interactions in single-stranded RNA and those of ds-DNA interactions with other external molecules have been performed using Raman spectroscopy, more specifically, EC-SERS,^[79–81] although some *in situ* FTIR spectroelectrochemical data are also available. In their study of RNA molecules on a glassy carbon surface by *in situ* FTIR spectroelectrochemistry, Wang et al.^[82] described the spectral changes associated with the oxidation of purine, guanine, and adenine. An increase in the intensity of bands attributed to C=O and C=N bonds was observed simultaneously with the intensity loss of C–H and N–H bands, which reflected the disturbance of the purine ring in the product of nucleic acid oxidation. Moreover, the intensity increase of other bands associated with the vibrational modes of pyrimidine rings suggested the occurrence of an adsorptive process at high positive potentials. Besides, DNA molecules

are known to be strongly adsorbed on Au surfaces. Therefore, different techniques have been employed to investigate the origin of this interaction.^[83,84] This is not only important in the context of investigating the structural changes in DNA itself under different conditions, but also provides a simple platform for studies in which DNA is used as a probe for the detection of other molecules. Doneux and Fojt used *in situ* FTIR spectroelectrochemistry to probe DNA components, namely cytidine 5'-monophosphate (CMP) and cytidine, on an Au electrode.^[85] Adsorption and desorption processes were observed for both molecules, as follows from the increase and decrease in the negative and positive absorption bands in the subtractively normalized interfacial FTIR spectra recorded at different potentials. Comparison of the normalized FTIR spectra of different CMPs (i.e., CMPI, CMPII, and CMPIII) with CMP SNIFTIR spectra revealed that CMP adsorption at the Au surface occurs through the formation of a chemical bond between the N3 atom of the pyrimidine base and Au.

4. Small biomolecules as electron carriers

In general, biological systems are macromolecules produced by the bonding of monomers. For instance, a redox enzyme is a protein formed by the bonding of several kinds of amino acids. Other types of monomers are monosaccharides, nucleotides, and fatty acids, which can be considered as building blocks for the formation of more complex biosystems. These molecules, along with coenzymes, cofactors, and macrocyclic organic compounds, belong to the class of small biomolecules.

As mentioned previously, EPR spectroelectrochemistry has been successfully used to evaluate the formation of free radicals during enzymatic catalysis and identify the active center within the redox cofactors of several proteins such as heme proteins, flavoproteins, quinoproteins, and oxireductases.^[86–88] In metallic structures, the fluctuation between several stable oxidation states allows EPR-detectable electronic configurations with unpaired electrons. The free electrons or radical species can also be observed using this analytical technique. However, in the case of metals, electronic state relaxation requires measurements to be carried out at extremely low temperatures (e.g., 77 K for Cu- and 4 K for Fe-containing structures), which makes the application of *in situ* EPR spectroelectrochemistry in real time impossible. For carbon-based radicals, on the other hand, unpaired electrons can be detected at room temperature, as exemplified by an investigation of ET during the oxidation of ethanol bioelectrocatalyzed by ADH and mediated by oxygenated functional groups attached to the surface of a carbon electrode.^[89] Previous studies correlated the enhanced ET rate of NADH, which is the cofactor of this enzyme, with the presence of carbonyl groups in the form of quinones and carboxylic acids on the surface of carbon electrodes.^[90] Operando EPR spectroelectrochemistry (Figure 8A) revealed the role of surface quinone groups as an electrocatalyst through the observation of an increasing number of free unpaired electrons as a more oxidative overpotential was applied for NADH oxidation (Figure 8B). This trend demonstrated the involvement of an anion radical as an intermediate of the catalytic process, which leads to the increased catalytic capability of quinone-enriched carbon surfaces (Figure 8C).

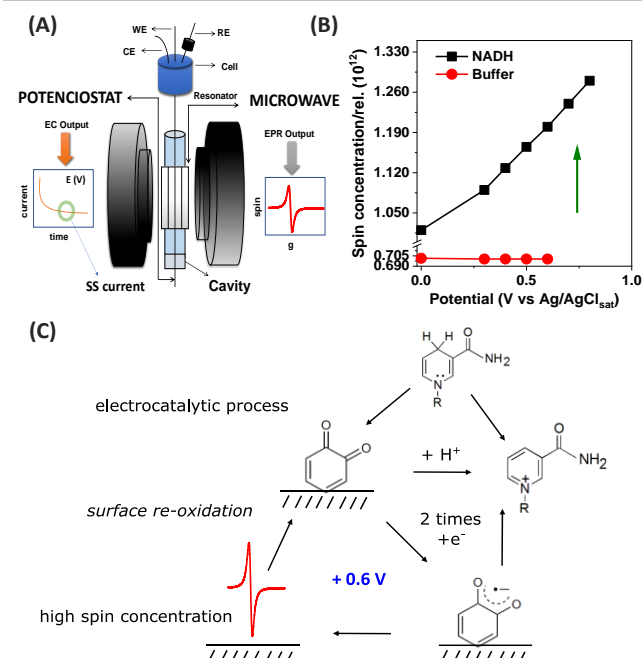


Figure 8. (A) *Operando* EPR cell design for electrochemical applications. (B) Relative spin concentration as function of the applied potential in the presence and absence of NADH. (C) Proposed mechanism that generates an anion radical as an intermediate observed by *operando* EPR spectroscopy. Reprinted from Ref. 90 with permission from the American Chemical Society, 2019.

EC-SERS has been used to monitor molecular-level changes due to the interactions between a model amyloid-forming protein (insulin) and a biomimetic membrane under biologically relevant electric fields.^[91] Various insulin structures interact with a model biomembrane system in different ways were detected along the aggregation pathway. Raman spectra recorded at open-circuit potential (OCP) indicated the presence of oligomers and protofibrils, which caused most of the membrane perturbation and were therefore the most likely candidates for cell toxicity and death. Such studies are crucial for a comprehensive understanding of the pathophysiology of Alzheimer's disease and the development of future therapeutics. In another example, EC-resonance Raman spectroscopy was used to investigate the catalytic intermediates formed during decaheme cytochrome-catalyzed H_2O_2 reduction.^[92] The results showed that most heme groups in the cytochrome are redox-active and are reduced upon the application of a cathodic potential, suggesting the formation of high-valence Fe oxo species as the catalytic intermediates of H_2O_2 reduction.

Electrochemical tip-enhanced Raman scattering (EC-TERS) microscopy is an emerging technique that combines scanning probe microscopy with Raman spectroscopy under electrochemical control conditions and is therefore well suited for probing redox reactions.^[93,94] However, this technique has not yet been applied to bioelectrochemical systems. As a proof of concept, Sabanés et al.^[95] monitored the EC-TERS response of an adenine monolayer adsorbed on an Au crystal and thus accessed the vibrational fingerprints of less than 100 molecules adsorbed at atomically flat Au electrodes to study the adsorption geometry and chemical reactivity as a function of applied potential (Figure 9). With increasing potential, the molecules adopted a flat adsorption geometry with strong Au–N interactions between deprotonated adenine molecules and the substrate.

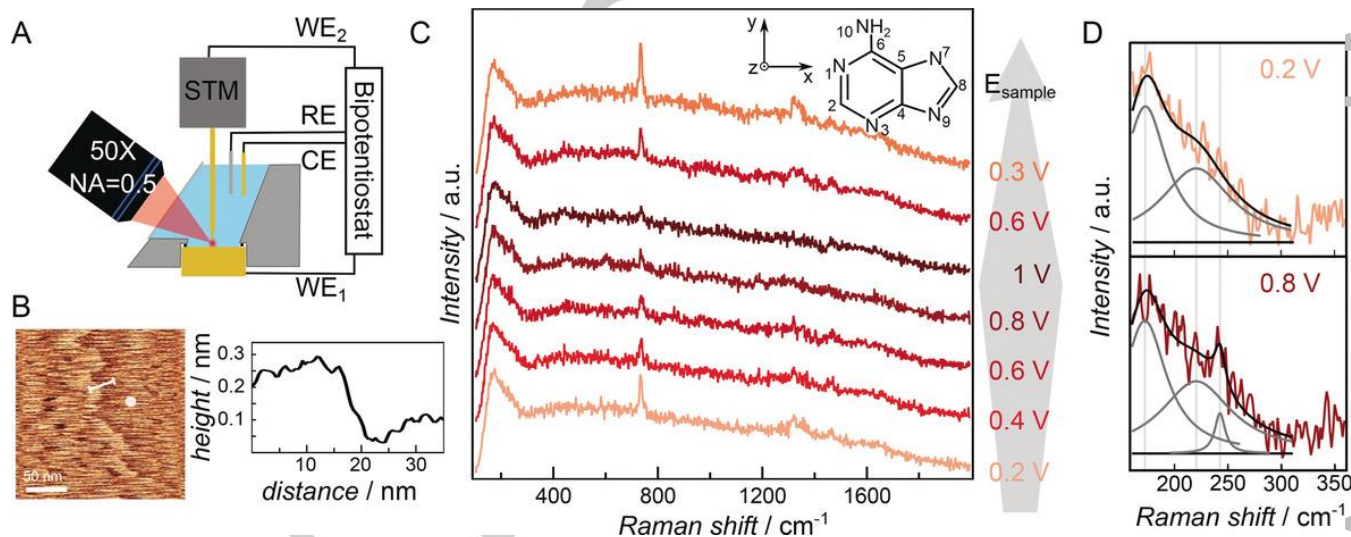


Figure 9. (A) EC-TERS cell and electrode configuration; STM = scanning tunneling microscope; WE/CE/RE = working/counter/reference electrode. (B) Left: STM image ($E_{\text{sample}} = 0.5 \text{ V}$, $E_{\text{bias}} = 0.4 \text{ V}$, $I_t = 1.35 \text{ nA}$); dot indicates EC-TERS sampling position. Right: Au step line profile as indicated in STM image. (C) EC-TERS spectral evolution upon WE1 potential ramp. Inset: neutral adenine. (D) Lorentzian band fitting examples for the low-wavenumber region. Reprinted from Ref. 95 with permission from Wiley-VCH, 2017.

REVIEW

WILEY-VCH

5. Bio-spectroelectrochemistry through membranes and cells

Cells, as the most basic biological functional units, are complex entities interacting with diverse biomolecules firstly through their membranes,^[96] which mainly comprise lipid molecules assembled in a well-structured thin bilayer that forms the outer boundary of living cells.^[97] These lipids can be roughly divided into three major classes, namely phospholipids, glycolipids, and sterols,^[98] and act as a highly selective barrier between the intracellular and extracellular environments.^[97,99] Biomembranes can incorporate numerous kinds of biomolecules such as proteins, saccharides, and carbohydrates, which have crucial roles, e.g., are involved in the operation of transmembrane ion-conducting channels, signaling receptors, active transporters, compartmentalization and adhesion processes, and cell-cell recognition.^[100,101]

Understanding the formation of lipid membranes as well as their structure, dynamics, and influence on the mechanisms of membrane-embedded enzyme-catalyzed reactions is of ultimate importance to chemistry, physics, biology, medicine, and technology.^[100,102] The investigation of highly oriented ET pathways in these systems, such as those in the ET chain, is also important, as they are involved in bioenergetics and cell metabolism. However, the intrinsic complexity of such pathways occasionally prevents direct access to these features *in vivo*, which has motivated the development of model membranes such as liposomes, Langmuir-Blodgett films, and supported lipid bilayers.^[103] The major advantage of these simplified biomimetic systems is the possibility to directly correlate their physical properties and processes with those of natural biological membranes and living cells themselves.^[104]

IR spectroscopy is a well-established method used to study interactions between lipid membranes and biomolecules, as IR spectra can be obtained for a wide range of environments without the need for probe molecules.^[105] To this end, two different data acquisition methods are commonly employed, namely ATR-FTIR and polarization modulation-IRRAS (PM-IRRAS) spectroscopy

. ATR-FTIR was used to study the interactions of cytochrome c with cardiolipin-containing membranes supported on functionalized Au electrodes,^[106] as the understanding of these interactions can lead to a better comprehension of cell apoptotic mechanisms. Studies concerning the elucidation of redox processes of membrane-embedded enzymes are still limited in comparison to those of globular enzymes. The main reason for this is related to the difficulties of developing electrodes that mimic the native membrane environment essential for the functioning of these enzymes.^[107] SEIRA spectroelectrochemistry has proven to be of great use to address this limitation. Wiebalck et al.^[108] reported catalytic O₂ reduction and the formation of a transmembrane proton gradient in a ubiquinol/cytochrome b₅ (cyt b₅) couple incorporated into a tethered bilayer lipid membrane (tBLM) on Au substrate (Fig. 10A). The authors used SEIRA-spectroscopic redox titration (Fig. 10B) to correlate shifts in the pH-dependent redox potential of ubiquinones (DUQ) under turnover conditions (Figure 10C) with the alkalization of the submembrane aqueous reservoir, which is the interface at which the electrode-ubiquinone/ubiquinol ET takes place. This approach has great potential for monitoring enzymatic and bioenergetic processes at electrode interfaces.

PM-IRRAS is used to study solid-liquid interfaces in aqueous environments. In this case, the incident IR beam passes through the solution and is reflected at the supported solid surface on which the membrane has been formed.^[109] The technique provides information regarding the conformation, orientation, and hydration of biomembranes. For instance, PM-IRRAS allows the investigation of how water cushion formation separates a phospholipid bilayer from the electrode surface influencing the membrane orientation and ET processes.^[110,111] Capacitance and chronocoulometric measurements coupled with PM-IRRAS are effective for probing the stability of the lipid monolayer on electrodes and determining the conformation and orientation of acyl chains as a function of applied potentials^[112–114] as well as for studying ion channel properties, lipid-peptide interactions, and transmembrane ion transport mechanisms.^[115–117] Recently, Su et al.^[115] applied electrochemical impedance spectroscopy (EIS) and *in situ* PM-IRRAS to probe the ion-channel properties of colicin E1 (a channel-forming protein incorporated into a floating lipid bilayer) as a function of transmembrane potential. EIS data showed that bilayer resistance decreased as the potential became more negative, while PM-IRRAS results indicated that the α -helix tilt angle of colicin E1 also decreased at negative transmembrane potentials, which indicated α -helix insertion into the biomembrane and the formation of ion channels therein.

UV-vis spectroscopy is another technique frequently used to gain information on bioelectrochemical systems, especially on the interaction of biomolecules (containing UV-vis-active groups) and lipid membranes. For instance, this approach was used to study the interaction of baicalein, a flavonoid, with a supported lipid bilayer membrane (s-BLM) to screen for the bioactivity of this drug and its passive diffusion through the biomembrane.^[118] The electrochemical results showed that baicalein can introduce defects into the s-BLM, while UV-vis measurements indicated that this molecule can insert itself into the BLM core. The above technique was also used to monitor the *in situ* ET between cytochrome c and iron oxide nanoparticles incorporated in a cell model biomembrane. The results indicated that these nanoparticles act as non-proteinaceous complexes III and IV of the mitochondrial respiratory chain, mimicking their redox properties in a bioinspired system, as evidenced by characteristic changes in the electronic absorption spectra of the protein.^[119]

Similar to IR spectroscopy, Raman spectroscopy has been extensively used to obtain information concerning living cells and biomembranes, offering the benefits of rapid signal acquisition, spectral richness, and relatively low cost.^[120] SERS has been competitive in the investigation of biological samples, providing information on molecular structure and chemical composition.^[121] For example, the interaction between a model

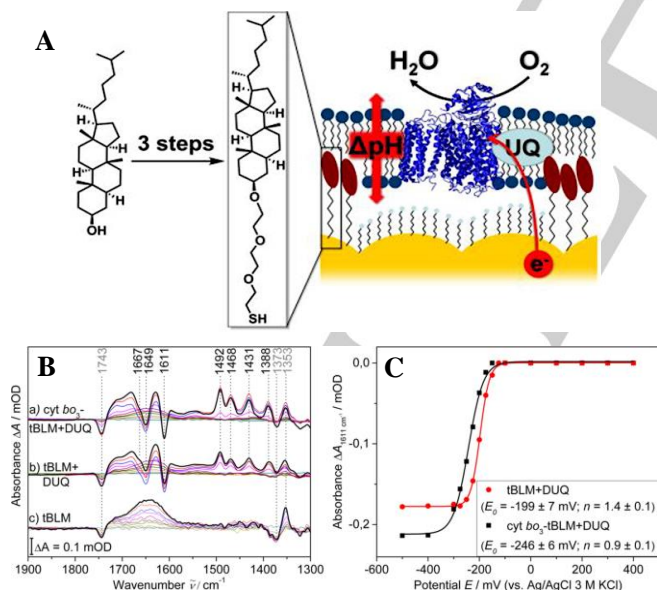


Figure 10. (A) Representation of the ubiquinol/cyt b₅ couple incorporated into a tBLM. (B) Potential-dependent SEIRA difference spectra recorded for the reduction of cyt b₅-tBLM+DUQ under turnover conditions (with O₂) and those recorded for tBLM+DUQ and pure tBLMs (with Ar) taking the spectrum of +400 mV as reference. Colors refer to the following potentials: -500 mV (●); -400 mV (●); -300 mV (●); -200 mV (●); -100 mV (●); 0 mV (●); 100 mV (●); 200 mV (●); 300 mV (●); 400 mV (●). (C) Potential-dependent intensities of the 1611 cm⁻¹ difference band of DUQ extracted from potential-dependent SEIRA spectra (Fig. 10B). Lines represent Nernst fits. Reprinted with permission from Ref. 108.

REVIEW

WILEY-VCH

protein aggregate and a biomimetic membrane was studied using EC-SERS to monitor the molecular-level changes due to this interaction.^[91] The same approach was used to monitor potential-driven changes in model biological membranes deposited on highly ordered nanocavity-patterned Ag electrodes.^[122] SERS has also been applied to the study of living cells and microorganisms. Lynk et al.^[123] used EC-SERS for bacterial screening, realizing the detection and discrimination of Gram-positive (*E. coli*) and Gram-negative (*B. megaterium*) bacteria immobilized on a carbon screen-printed electrode (SPE) coated with AgNPs. The authors observed that the SERS signals for both bacteria gained intensity upon the application of a negative potential, with the strongest signal observed at -1.0 V. Figure 11A shows the cathodic progression of the SERS spectra for *B. megaterium*, while Figure 11B displays the evolution of the signal upon going from normal EC-SERS conditions (in air) to -1.0 V for *B. megaterium*. Scanning electron microscopy (SEM) imaging (Figure 11C) confirmed the presence of *B. megaterium* on the AgNP-coated surface of the SPE. The EC-SERS data were compared with those for *E. coli* to differentiate between the two strains of bacteria.

Fluorescence spectroscopy coupled with an electrochemical method was used to examine the transport of an ionic substance through a bilayer lipid membrane.^[124] Transport across membranes was examined by simultaneously measuring the transmembrane current and fluorescence intensity as a function of the applied membrane potential. This finding is of great importance for understanding biomembrane-related phenomena such as neurotransmission and respiration as well as the delivery of ionic drugs into the cell. Fluorescence spectroelectrochemical measurements were also used to evaluate the extracellular electron transfer (EET) of electrochemically active microbial biofilms and the potential-dependent conformational changes in redox enzymes involved in these processes.^[125] In addition, this technique provides information on the chemical nature and kinetic parameters of EET components.

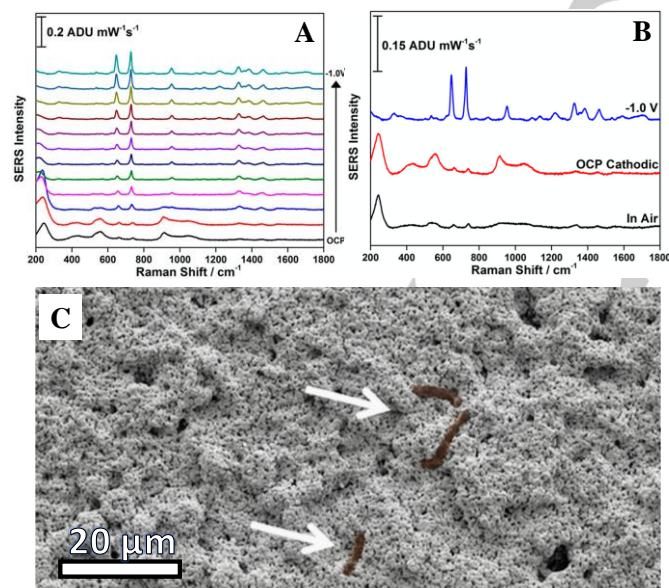


Figure 11. (A) EC-SERS signal for *B. megaterium* on AgNPs at OCP and the cathodic progression from 0.0 V to -1.0 V in 100-mV increments. (B) Comparison of the EC-SERS spectrum collected in air with those collected at OCP and -1.0 V. Data were collected using a 780-nm laser at a laser power of 80 mW and an acquisition time of 30 s. (C) SEM image recorded at 5.0 kV showing the surface of AgNPs coated with *B. megaterium* cells. Arrows indicate the location of bacterial cells (colored brown). Reprinted with permission from Ref. 123.

AFM is a local-probe microscopy method sensing interactions between an atomically sharp tip and the sample surface via the electronic clouds on external atoms. AFM is well

suited for biological sample characterization, as it can be performed in aqueous solutions under physiological conditions, in real time, and at high resolution, allowing the acquisition of structural images and the characterization of interaction forces, elasticity, and chemical properties.^[100] AFM has been coupled with different techniques such as fluorescence and Raman spectroscopy as well as electrochemical methods. In the field of coupled electrochemical methods, atomic force-scanning electrochemical microscopy (AFM-SECM) is commonly used for the *in situ* identification and structural characterization of individual virus particles and the mapping of protein distribution inside the same.^[126] Knittel et al.^[127] modified conductive colloid AFM-SECM probes with polystyrene sulfonate and poly(3,4-ethylenedioxythiophene) to use them for single-cell force measurements in mouse fibroblasts and investigate single-cell interactions under different applied electric potentials. This approach has been used as a bioanalytical technique for monitoring cellular homeostasis through the evaluation of living cell membrane permeability to a series of compounds such as toxic heavy metals.^[128–130] AFM-SECM is also useful for the study of living single-cell microorganisms such as bacteria, providing insights into metabolic exchange between two different bacteria^[131] or even furnishing information on the efficiency of charge transfer from yeast cells under anaerobic conditions.^[132] This approach was employed by Nebel et al.^[133] to visualize oxygen consumption (and the respiration activity itself) in living cells, which is an important result, as it indicates cell metabolic vitality. Investigations of cytomembrane permeability can be carried out using biomimetic membrane surfaces, as shown by Huang et al.,^[134] who used AFM-SECM to probe the reversible cationic switchable properties of a self-assembled monolayer and showed that the homogeneous monolayer features a uniform distribution of switch molecules (11-mercaptoundecanoic acid). The above approach was also used to probe the incorporation of a channel-forming protein (C2IIa) and the transport of a metal complex through these cationic-sensitive channels.^[135]

6. Summary and outlook

In view of their ability to simultaneously monitor ET and the associated changes in the molecular structure of biological systems, *in situ* and *operando* electrochemistry techniques offer unprecedented advantages for identifying the active catalytic centers of biomolecules, elucidating the mechanisms of complex reaction pathways, and providing insights into the thermodynamic and kinetic parameters. Analysis of the most recently reported data demonstrates the importance of this technique for the investigation of complex biological entities ranging from small biomolecules (such as coenzymes) to entire cells. These investigations supply important information for a wide range of research fields and provide fundamental biochemical parameters that are of great significance for basic sciences and can be used to develop new technologies such as biosensors for the diagnosis and development of more efficient drugs. *Operando* electrochemistry is a state-of-the-art approach for the elucidation of enzymatic reaction mechanisms, as the redox state of the cofactor or coenzyme can be monitored by an electrochemical technique, while the products, reagents, and enzymatic conformational changes can be monitored by spectroscopic or spectrometric techniques. For instance, *operando* DEMS can be very helpful in the studies of CO₂ capture^[136,137] and NH₃ production^[138] by enzyme-catalyzed cascade reactions. Therefore, *operando* DEMS can be used to probe the action mechanisms of some enzymes, e.g., formate dehydrogenase, formaldehyde dehydrogenase, aldehyde dehydrogenase, and hydrogenases. Similarly, *in situ* vibrational spectroscopy allows one to correlate the bioelectrochemical activity of redox-active biomolecules to their structural changes,

REVIEW

WILEY-VCH

thus providing direct information on protein functions. The spectroelectrochemical techniques used in the study of nucleic acids can provide detailed information on the carcinogenesis mechanism, as DNA damage is involved in this process. The future development of *in situ* and *operando* spectroelectrochemistry should be focused on improving temporal and spatial resolution to increase the sensitivity of the coupled technique for single-molecule detection, as exemplified by nano-FTIR, tip-enhanced IR, and Raman spectroscopy. Furthermore, some others techniques, such as electrochemical quartz crystal microbalance (EQCM), surface plasmon resonance (SPR), and scanning electrochemical microscopy (SECM) are promising to bring a better explanation of the complex biological processes, which is essential for fabricating devices with enhanced biological function. Particularly, in the case of EQCM,^[139] the high sensitivity of this technique can be used for detecting small changes during the conformational changes of the proteins and nucleic acids.

Acknowledgements

The authors gratefully acknowledge the São Paulo Research Foundation (FAPESP; grant nos. 15/22973-6, 17/20493-2 19/15333-1, 19/12053-8, and 18/22214-6), the Coordinating Agency for Advanced Training of Graduate Personnel (CAPES; grant no. 88887.358060/2019-00), the MeDiCo Network CAPES-Brazil (grant no. 88881.504532/2020-01), and the National Council of Scientific and Technological Development (CNPq; project nos. 305486/2019-5 and 134396/2018-9) for financial support.

Keywords: • biocatalysis • electron transfer • *in situ* electrochemistry • *operando* electrochemistry • spectroelectrochemistry

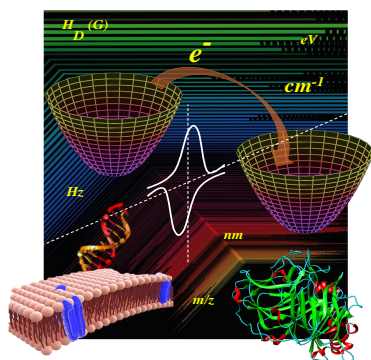
- [1] K. J. Lee, N. Elgrishi, B. Kandemir, J. L. Dempsey, *Nat. Rev. Chem.* **2017**, 1, 0039.
- [2] Weckhuysen, B. M. *Phys. Chem. Chem. Phys.* **2003**, 5, No. vi.
- [3] Cuisinier, M., Cabelguen, P. E., Evers, S., He, G., Kolbeck, M., Garsuch, A., Bolin, T., Balasubramanian, M. Nazar, L. F., *J. Phys. Chem. Lett.*, **2013**, 4, 3227-3232.
- [4] L. J. A. Macedo, F. N. Crespilho, *Anal. Chem.* **2018**, 90, 1487–1491.
- [5] L. J. A. Macedo, A. Hassan, G. C. Sedenho, F. N. Crespilho, *Nat. Commun.* **2020**, 11, 316..
- [6] R. F. Savinell, K. Ota, G. Kreysa, *Encyclopedia of Applied Electrochemistry*, Springer, New York, **2014**.
- [7] B. Sharma, R. R. Frontiera, A. I. Henry, E. Ringe, R. P. van Duyne, *Mater. Today* **2012**, 15, 16–25.
- [8] A. M. Beale, G. Sankar, C. R. A. Catlow, P. A. Anderson, T. L. Green, *Phys. Chem. Chem. Phys.* **2005**, 7, 1856–1860.
- [9] D. M. Murphy, *EPR (Electron Paramagnetic Resonance) Spectroscopy of Polycrystalline Oxide Systems*, John Wiley & Sons, Weinheim, **2009**.
- [10] R. J. Gale, *Spectroelectrochemistry: Theory and Practice*, Springer Science & Business Media, New York, **2012**.
- [11] R. M. Teeling-Smith, Y. W. Jung, N. Scozzaro, J. Cardellino, I. Rampersaud, J. A. North, M. Simon, V. P. Bhallamudi, A. Rampersaud, E. Johnston-Halperin, M. G. Poirier, P. C. Hammel, *Biophys. J.* **2016**, 110, 2044–2052.
- [12] I. D. Sahu, R. M. McCarrick, G. A. Lorigan, *Biochemistry* **2013**, 52, 5967–5984.
- [13] K. E. Prosser, C. J. Walsby, *Eur. J. Inorg. Chem.* **2017**, 2017, 1573–1585.
- [14] M. A. Tamski, J. v. MacPherson, P. R. Unwin, M. E. Newton, *Phys. Chem. Chem. Phys.* **2015**, 17, 23438–23447.
- [15] D. T. Petasis, M. P. Hendrich, *Quantitative Interpretation of Multifrequency Multimode EPR Spectra of Metal Containing Proteins, Enzymes, and Biomimetic Complexes*, Elsevier, New York, **2015**.
- [16] V. B. Arion, P. Raptá, J. Telser, S. S. Shova, M. Breza, K. Lušpai, J. Kožisek, *Inorg. Chem.* **2011**, 50, 2918–2931.
- [17] M. Comtat, H. Durlat, *Biosens. Bioelectron.* **1994**, 9, 663–668.
- [18] Ł. Krzeminski, L. Ndamba, G. W. Canters, T. J. Aartsma, S. D. Evans, L. J. C. Jeuken, *J. Am. Chem. Soc.* **2011**, 133, 15085–15093.
- [19] J. M. Salverda, A. v. Patil, G. Mizzon, S. Kuznetsova, G. Zauner, N. Akklic, G. W. Canters, J. J. Davis, H. A. Heering, T. J. Aartsma, *Angew. Chem. Int. Ed.* **2010**, 49, 5776–5779.
- [20] S. P. Wu, M. Bellei, S. S. Mansy, G. Battistuzzi, M. Sola, J. A. Cowan, *J. Inorg. Biochem.* **2011**, 105, 806–811.
- [21] Y. Zhu, G. Cheng, S. Dong, *Biophys. Chem.* **2002**, 97, 129–138.
- [22] A. B. Chinen, C. M. Guan, J. R. Ferrer, S. N. Barnaby, T. J. Merkel, C. A. Mirkin, *Chem. Rev.* **2015**, 115, 10530–10574.
- [23] A. B. T. Ghisaidoobe, S. J. Chung, *Int. J. Mol. Sci.* **2014**, 15, 22518–22538.
- [24] J. C. P. de Souza, W. O. Silva, F. H. B. Lima, F. N. Crespilho, *Chem. Commun.* **2017**, 53, 8400–8402.
- [25] W. A. El-Said, T. H. Kim, Y. H. Chung, J. W. Choi, *Biomaterials* **2015**, 40, 80–87.
- [26] M. Holzinger, A. le Goff, S. Cosnier, *New J. Chem.* **2014**, 38, 5173–5180.
- [27] D. H. Murgida, P. Hildebrandt, *Phys. Chem. Chem. Phys.* **2005**, 7, 3773–3784.
- [28] Á. I. López-Lorente, C. Kranz, *Curr. Opin. Electrochem.* **2017**, 5, 106–113.
- [29] J. T. Li, Z. Y. Zhou, I. Broadwell, S. G. Sun, *Acc. Chem. Res.* **2012**, 45, 485–494.
- [30] P. L. Fale, A. Altharawi, K. L. A. Chan, *Biochim. Biophys. Acta, Mol. Cell Res.* **2015**, 1853, 2640–2648.
- [31] P. A. Ash, K. A. Vincent, *Chem. Commun.* **2012**, 48, 1400–1409.
- [32] D. Millo, P. Hildebrandt, M. E. Pandelia, W. Lubitz, I. Zebger, *Angew. Chem. Int. Ed.* **2011**, 50, 2632–2634.
- [33] D. Millo, P. Hildebrandt, M. E. Pandelia, W. Lubitz, I. Zebger, P. A. Ash, K. A. Vincent, *Angew. Chem. Int. Ed.* **2012**, 50, 1400–1409.
- [34] M. Fedurco, *ChemInform* **2010**, 32, numeros de paginas.
- [35] K. Ataka, J. Heberle, *J. Am. Chem. Soc.* **2004**, 126, 9445–9457.
- [36] P. Paengnakorn, P. A. Ash, S. Shaw, K. Danyal, T. Chen, D. R. Dean, L. C. Seefeldt, K. A. Vincent, *Chem. Sci.* **2017**, 8, 1500–1505.
- [37] R. Hidalgo, P. A. Ash, A. J. Healy, K. A. Vincent, *Angew. Chem. Int. Ed.* **2015**, 54, 7110–7113.
- [38] J. Kozuch, C. Weichbrodt, D. Millo, K. Giller, S. Becker, P. Hildebrandt, C. Steinem, *Phys. Chem. Chem. Phys.* **2014**, 16, 9546–9555.
- [39] J. J. Leitch, C. L. Brosseau, S. G. Roscoe, K. Bessonov, J. R. Dutcher, J. Lipkowsky, *Langmuir* **2013**, 29, 965–976.
- [40] T. Kobori, S. Iwamoto, K. Takeyasu, T. Ohtani, *Biopolymers* **2007**, 85, 392–406.
- [41] P. A. Ash, S. E. T. Kendall-Price, K. A. Vincent, *Acc. Chem. Res.* **2019**, 52, 3120–3131.
- [42] J. Kozuch, C. Steinem, P. Hildebrandt, D. Millo, *Angew. Chem. Int. Ed.* **2012**, 51, 8114–8117.
- [43] X. Jiang, E. Zaitseva, M. Schmidt, F. Siebert, M. Engelhard, R. Schlesinger, K. Ataka, R. Vogel, J. Heberle, *Proc. Natl. Acad. Sci. U. S. A.* **2008**, 105, 12113–12117.
- [44] P. Rodríguez-Maciá, K. Pawlak, O. Rüdiger, E. J. Reijerse, W. Lubitz, J. A. Birrell, *J. Am. Chem. Soc.* **2017**, 139, 15122–15134.
- [45] C. di Bari, N. Mano, S. Shleev, M. Pita, A. L. De Lacey, *J. Biol. Inorg. Chem.* **2017**, 22, 1179–1186.
- [46] A. Hassan, L. J. A. Macedo, J. C. P. de Souza, F. C. D. A. Lima, F. N. Crespilho, *Sci. Rep.* **2020**, 10, 1–12.
- [47] Y. el Khoury, P. Hellwig, *ChemPhysChem* **2011**, 12, 2669–2674.
- [48] L. Marboutin, H. Petitjean, B. Xerri, N. Vita, F. Dupeyrat, J. P. Flament, D. Berthomieu, C. Berthomieu, *Angew. Chem. Int. Ed.* **2011**, 50, 8062–8066.
- [49] J. E. Penner-Hahn, *Compr. Coord. Chem. II* **2003**, 2, 159–186.
- [50] B. Sharma, R. R. Frontiera, A. I. Henry, E. Ringe, R. P. van Duyne, P. A. Ash, R. Hidalgo, K. A. Vincent, *ACS Catal.* **2012**, 7, 16–25.
- [51] I. Ascone, W. Meyer-Klaucke, L. Murphy, *J. Synchrotron Radiat.* **2003**, 10, 16–22.
- [52] A. A. Hummer, A. Rempel, *X-Ray Absorption Spectroscopy: A Tool to Investigate the Local Structure of Metal-Based Anticancer Compounds In Vivo*, Elsevier, Kidlington (Oxford), **2013**.
- [53] M. Ranieri-Raggi, A. Raggi, D. Martini, M. Benvenuto, S. Mangai, *J. Synchrotron Radiat.* **2003**, 10, 69–70.
- [54] J. E. Penner-Hahn, *Coord. Chem. Rev.* **2005**, 249, 161–177.
- [55] I. J. Pickering, R. C. Prince, T. Divers, G. N. George, *FEBS Lett.* **1998**, 441, 11–14.
- [56] R. Ortega, A. Carmona, I. Llorens, P. L. Solari, *J. Anal. At. Spectrom.* **2012**, 27, 2054–2065.
- [57] A. Arcovito, M. Benfatto, M. Ciani, S. S. Hasnain, K. Nienhaus, G. U. Nienhaus, C. Savino, R. W. Strange, B. Vallone, S. della Longa, *Proc. Natl. Acad. Sci. U. S. A.* **2007**, 104, 6211–6216.
- [58] R. W. Strange, M. C. Feiters, *Curr. Opin. Struct. Biol.* **2008**, 18, 609–616.
- [59] B. M. Gibbons, M. Wette, M. B. Stevens, R. C. Davis, S. Siahrostami, M. Kreider, A. Mehta, D. C. Higgins, B. M. Clemens, T. F. Jaramillo, *Chem. Mater.* **2020**, 32, 1819–1827.
- [60] S. Song, J. Zhou, X. Su, Y. Wang, J. Li, L. Zhang, G. Xiao, C. Guan, R. Liu, S. Chen, H. J. Lin, S. Zhang, J. Q. Wang, *Energy Environ. Sci.* **2018**, 11, 2945–2953.
- [61] H. Koga, L. Croguennec, M. Ménétrier, P. Mannessiez, F. Weill, C. Delmas, S. Belin, *J. Phys. Chem. C* **2014**, 118, 5700–5709.
- [62] M. V. Varsha, G. Nageswaran, *Front. Chem.* **2020**, 8, DOI 10.3389/fchem.2020.00023.

REVIEW

WILEY-VCH

- [63] B. Lassalle-Kaiser, S. Gul, J. Kern, V. K. Yachandra, J. Yano, *J. Electron Spectrosc. Relat. Phenom.* **2017**, 221, 18–27.
- [64] M. Wang, L. Árnadóttir, Z. J. Xu, Z. Feng, *Nano-Micro Lett.* **2019**, 11, 1–18.
- [65] T. Glaser, B. Hedman, K. O. Hodgson, E. I. Solomon, *Acc. Chem. Res.* **2000**, 33, 859–868.
- [66] K. Abdiaziz, E. Salvadori, M. M. Roessler, E. Reisner, *Chem. Commun.* **2019**, 8840–8843.
- [67] P. C. Hanawalt, G. Spivak, *Nat. Rev. Mol. Cell Biol.* **2008**, 9, 958–970.
- [68] M. Scofield, *xPharm: The Comprehensive Pharmacology Reference*, Elsevier, Amsterdam, **2007**, pp. 1–15.
- [69] F. Bleichert, M. R. Botchan, J. M. Berger, *Science* **2017**, 355, eaah6317.
- [70] E. T. Kool, *Annu. Rev. Biophys. Biomol. Struct.* **2001**, 30, 1–22.
- [71] J. L. Mergny, L. Lacroix, *Oligonucleotides* **2003**, 13, 515–537.
- [72] M. C. Williams, J. R. Wenner, I. Rouzina, V. A. Bloomfield, *Biophys. J.* **2001**, 80, 874–881.
- [73] A. Tempestini, V. Cassina, D. Brogioli, R. Ziano, S. Erba, R. Giovannoni, M. G. Cerrito, D. Salerno, F. Mantegazza, *Nucleic Acids Res.* **2013**, 41, 2009–2019.
- [74] S. N. Syed, H. Schulze, D. MacDonald, J. Crain, A. R. Mount, T. T. Bachmann, *J. Am. Chem. Soc.* **2013**, 135, 5399–5407.
- [75] R. A. Karaballi, A. Nel, S. Krishnan, J. Blackburn, C. L. Brosseau, *Phys. Chem. Chem. Phys.* **2015**, 17, 21356–21363.
- [76] D. Ibañez, A. Santidrian, A. Heras, M. Kalbáč, A. Colina, *J. Phys. Chem. C* **2015**, 119, 8191–8198.
- [77] Y. U. Kayran, N. Cinar, D. Jambrec, W. Schuhmann, *ChemElectroChem* **2018**, 5, 756–760.
- [78] B. Y. Wen, X. Jin, Y. Li, Y. H. Wang, C. Y. Li, M. M. Liang, R. Panneerselvam, Q. C. Xu, D. Y. Wu, Z. L. Yang, J. F. Li, Z. Q. Tian, *Analyst* **2016**, 141, 3731–3736.
- [79] D. K. Corrigan, N. Gale, T. Brown, P. N. Bartlett, *Angew. Chem. Int. Ed.* **2010**, 49, 5917–5920.
- [80] E. Papadopoulou, N. Gale, S. A. Goodchild, D. W. Cleary, S. A. Weller, T. Brown, P. N. Bartlett, *Chem. Sci.* **2015**, 6, 1846–1852.
- [81] B. Y. Wen, X. Jin, Y. Li, Y. H. Wang, C. Y. Li, M. M. Liang, R. Panneerselvam, Q. C. Xu, D. Y. Wu, Z. L. Yang, J. F. Li, Z. Q. Tian, *Analyst* **2016**, 141, 3731–3736.
- [82] Z. Wang, D. Liu, S. Dong, *Bioelectrochemistry* **2001**, 53, 175–181.
- [83] R. P. Johnson, J. A. Richardson, T. Brown, P. N. Bartlett, *J. Am. Chem. Soc.* **2012**, 134, 14099–14107.
- [84] L. A. Gearheart, H. J. Ploehn, C. J. Murphy, *J. Phys. Chem. B* **2001**, 105, 12609–12615.
- [85] T. Doneux, L. Folt, *ChemPhysChem* **2009**, 10, 1649–1655.
- [86] J. W. Whittaker, *Chem. Rev.* **2003**, 103, 2347–2363.
- [87] P. Hellwig, T. Yano, T. Ohnishi, R. B. Gennis, *Biochemistry* **2002**, 41, 10675–10679.
- [88] T. Ohnishi, *Biochim. Biophys. Acta, Bioenerg.* **1998**, 1364, 186–206.
- [89] A. R. Pereira, J. C. P. de Souza, A. D. Gonçalves, K. C. Pagnoncelli, F. N. Crespiho, *J. Braz. Chem. Soc.* **2017**, 28, 1698–1707.
- [90] M. A. Ali, A. Hassan, G. C. Sedenho, R. v. Gonçalves, D. R. Cardoso, F. N. Crespiho, *J. Phys. Chem. C* **2019**, 123, 16058–16064.
- [91] R. A. Karaballi, S. Merchant, S. R. Power, C. L. Brosseau, *Phys. Chem. Chem. Phys.* **2018**, 20, 4513–4526.
- [92] B. Reuillard, K. H. Ly, P. Hildebrandt, L. J. C. Jeuken, J. N. Butt, E. Reisner, *J. Am. Chem. Soc.* **2017**, 139, 3324–3327.
- [93] M. Mattei, G. Kang, G. Goubert, D. v. Chulhai, G. C. Schatz, L. Jensen, R. P. van Duyne, *Nano Lett.* **2017**, 17, 590–596.
- [94] Z. Chen, S. Jiang, G. Kang, D. Nguyen, G. C. Schatz, R. P. van Duyne, *J. Am. Chem. Soc.* **2019**, 141, 15684–15692.
- [95] N. Martín Sabanés, T. Ohto, D. Andrienko, Y. Nagata, K. F. Domke, *Angew. Chem. Int. Ed.* **2017**, 56, 9796–9801.
- [96] G. Huang, F. Li, X. Zhao, Y. Ma, Y. Li, M. Lin, G. Jin, T. J. Lu, G. M. Genin, F. Xu, *Chem. Rev.* **2017**, 117, 12764–12850.
- [97] R. Guidelli, *Bioelectrochemistry of Biomembranes and Biomimetic Membranes*, Wiley Online Library, **2017**.
- [98] X. Cheng, J. C. Smith, *Chem. Rev.* **2019**, 119, 5849–5880.
- [99] A. Mashaghi, S. Mashaghi, I. Reviakine, R. M. A. Heeren, V. Sandoghdar, M. Bonn, *Chem. Soc. Rev.* **2014**, 43, 887–900.
- [100] A. N. Bondar, M. J. Lemieux, *Chem. Rev.* **2019**, 119, 6162–6183.
- [101] T. H. Lee, D. J. Hirst, K. Kulkarni, M. P. del Borgo, M. I. Aguilar, *Chem. Rev.* **2018**, 118, 5392–5487.
- [102] F. A. Heberle, G. Pabst, *Biophys. Rev.* **2017**, 9, 353–373.
- [103] C. Sebaaly, H. Greige-Gerges, C. Charcosset, *Current Trends and Future Developments on (Bio-) Membranes: Membrane Processes in the Pharmaceutical and Biotechnological Field*, Elsevier, Amsterdam, **2018**, pp. 311–340.
- [104] Z. F. Su, J. J. Leitch, J. Lipkowski, *Curr. Opin. Electrochem.* **2018**, 12, 60–72.
- [105] H. Li, T. Zhao, Z. Sun, *Rev. Anal. Chem.* **2018**, 37, 1–23.
- [106] L. Zeng, L. Wu, L. Liu, X. Jiang, *Anal. Chem.* **2016**, 88, 11727–11733.
- [107] T. Laftoglou, L. J. C. Jeuken, *Chem. Commun.* **2017**, 53, 3801–3809.
- [108] S. Wiebalck, J. Kozuch, E. Forbrig, C. C. Tzschucke, L. J. C. Jeuken, P. Hildebrandt, *J. Phys. Chem. B* **2016**, 120, 2249–2256.
- [109] L. Wu, X. Jiang, *Infrared Spectroscopy for Studying Plasma Membranes*, Springer, Singapore, **2017**.
- [110] D. Matyszewska, R. Bilewicz, Z. F. Su, F. Abbasi, J. J. Leitch, J. Lipkowski, *Langmuir* **2016**, 32, 1791–1798.
- [111] B. Khairalla, J. Juhaniwicz-Debinska, S. Sek, I. Brand, *Bioelectrochemistry* **2020**, 132, 107443.
- [112] J. Alvarez-Malmagro, Z. Su, J. Jay Leitch, F. Prieto, M. Rueda, J. Lipkowski, *Langmuir* **2019**, 35, 901–910.
- [113] E. Madrid, S. L. Horswell, *Langmuir* **2015**, 31, 12544–12551.
- [114] I. Brand, K. W. Koch, *Bioelectrochemistry* **2018**, 124, 13–21.
- [115] Z. Su, M. Shodiev, J. J. Leitch, F. Abbasi, J. Lipkowski, *Langmuir* **2018**, 34, 6249–6260.
- [116] Z. F. Su, M. Shodiev, J. Jay Leitch, F. Abbasi, J. Lipkowski, *J. Electroanal. Chem.* **2018**, 819, 251–259.
- [117] Z. F. Su, D. Ho, A. R. Merrill, J. Lipkowski, *Langmuir* **2019**, 35, 8452–8459.
- [118] Y. Zhang, X. Wang, L. Wang, M. Yu, X. Han, *Bioelectrochemistry* **2014**, 95, 29–33.
- [119] I. Modenez, L. Macedo, A. F. A. Melo, A. R. Pereira, O. N. Oliveira Junior, F. Crespiho, **2020**, DOI 10.26434/chemrxiv.12084006.
- [120] P. A. Mosier-Boss, *Biosensors* **2017**, 7, 51.
- [121] D. Volpati, P. H. B. Aoki, P. Alessio, F. J. Pavinatto, P. B. Miranda, C. J. L. Constantino, O. N. Oliveira, *Adv. Colloid Interface Sci.* **2014**, 207, 199–215.
- [122] M. Vezvaie, C. L. Brosseau, J. Lipkowski, *Electrochim. Acta* **2013**, 110, 120–132.
- [123] T. P. Lynk, C. S. Sit, C. L. Brosseau, *Anal. Chem.* **2018**, 90, 12639–12646.
- [124] T. Omatsu, K. Hori, Y. Naka, M. Shimazaki, K. Sakai, K. Murakami, K. Maeda, M. Fukuyama, Y. Yoshida, *Analyst* **2020**, 145, 3839–3845.
- [125] I. Schmidt, A. Pieper, H. Wichmann, B. Bunk, K. Huber, J. Overmann, P. J. Walla, U. Schröder, *ChemElectroChem* **2017**, 4, 2515–2519.
- [126] L. Nault, C. Taofifenua, A. Anne, A. Chovin, C. Demaille, J. Besong-Ndika, D. Cardinale, N. Carette, T. Michon, J. Walter, *ACS Nano* **2015**, 9, 4911–4924.
- [127] P. Knittel, H. Zhang, C. Kranz, G. G. Wallace, M. J. Higgins, *Nanoscale* **2016**, 8, 4475–4481.
- [128] F. P. Filice, M. S. M. Li, J. D. Henderson, Z. Ding, *Anal. Chim. Acta* **2016**, 908, 85–94.
- [129] J. D. Henderson, F. P. Filice, M. S. M. Li, Z. Ding, *ChemElectroChem* **2017**, 4, 856–863.
- [130] M. S. M. Li, F. P. Filice, J. D. Henderson, Z. Ding, *J. Phys. Chem. C* **2016**, 120, 6094–6103.
- [131] V. S. Joshi, P. S. Sheet, N. Cullin, J. Kreth, D. Koley, *Anal. Chem.* **2017**, 89, 11044–11052.
- [132] A. Ramanavicius, I. Morkvenaite-Vilkonciene, A. Kisieliute, J. Petroniene, A. Ramanaviciene, *Colloids Surf., B* **2017**, 149, 1–6.
- [133] M. Nebel, S. Grützke, N. Diab, A. Schulte, W. Schuhmann, *Angew. Chem. Int. Ed.* **2013**, 52, 6335–6338.
- [134] X. Huang, J. Chen, C. Yan, H. Shao, *Langmuir* **2019**, 35, 10772–10779.
- [135] C. M. Frey, A. Eifert, H. Schütz, H. Barth, B. Mizaikoff, C. Kranz, *Electrochim. Acta* **2016**, 209, 341–349.
- [136] R. Obert, B. C. Dave, *J. Am. Chem. Soc.* **1999**, 121, 12192–12193.
- [137] P. K. Addo, R. L. Arechederra, A. Waheed, J. D. Shoemaker, W. S. Sly, S. D. Minter, *Electrochem. Solid-State Lett.* **2011**, 14, 9–13.
- [138] M. Duca, J. R. Weeks, J. G. Fedor, J. H. Weiner, K. A. Vincent, *ChemElectroChem* **2015**, 2, 1086–1089.
- [139] Kornienko, N., Ly, K. H., Robinson, W. E., Heidary, N., Zhang, J. Z., & Reisner, E., *Acc. Chem. Res.*, **2019**, 52, 1439–1448.

Entry for the Table of Contents



Overview of *in situ* and *operando* electrochemistry techniques for studies of biological systems such as redox proteins, nucleic acids, small biomolecules, and biomembranes.

Institute and/or researcher Twitter usernames: @fcrespilho